

Unclassified Report  
Nat.Lab. Unclassified Report 003/96

**Parameter extraction  
methodology for the MEXTRAM  
bipolar transistor model**

Author(s): W.J. Kloosterman and J.A.M. Geelen

© *Philips Electronics N.V. 1996*  
*All rights are reserved. Reproduction in whole or in part is prohibited without the written consent of the copyright owner.*

---

<b>Unclassified Report:</b>	003/96
<b>Title:</b>	Parameter extraction methodology for the MEXTRAM bipolar transistor model
<b>Author(s):</b>	W.J. Kloosterman and J.A.M. Geelen

---

<b>Part of project:</b>	
<b>Customer:</b>	

---

<b>Keywords:</b>	Mextram; characterization, parameter extraction; bipolar; compact models;
<b>Abstract:</b>	Nowadays to predict circuit performance like optimization of high speed circuits, support for process development and parametric yield prediction, the use of CAD programs like Spice and Spectre is common practice. The reliability of these predictions mainly depend on a correct description of the circuitry, the accuracy and scalability of the electrical models of the circuit components. In general the accuracy of the electrical model increases with model complexity and unfortunately also the number of transistor model parameters increases. Therefore a robust and unambiguous parameter extraction methodology of transistor model parameters for advanced electrical models becomes a important issue. This report deals with the required measurements and parameter extraction methodology for the public domain state of the art MEXTRAM bipolar transistor model.

---

<b>Conclusions:</b>	A very fast and accurate parameter extraction method for the bipolar transistor model MEXTRAM has been developed. Using a combination of simplified expressions and selected measurements the iterative solution of the full model is avoided. The method is implemented in the parameter extraction software package IC-CAP of Hewlett-Packard. The complete MEXTRAM model is built into the MNS circuit simulator of HP and is interfaced with IC-CAP to calculate all transistor characteristics to be compared with measurements. The required measurements with bias conditions, initial parameter set and the parameter extraction strategy is explained. The different steps and the used simplified MEXTRAM relations involved are described. This new method greatly enhances the efficiency and user-friendliness of the MEXTRAM parameter extraction.
---------------------	--



# Contents

1	History of documentation	1
2	Introduction	1
3	Measurements	1
4	Initial parameter set	3
5	Parameter extraction strategy	7
6	Equivalent electrical circuit	9
7	Depletion Capacitances	10
8	Reverse Early effect	14
9	Forward Early effect	15
10	Avalanche	17
11	Collector saturation current	19
12	Forward current gain	19
13	Base series resistances	21
14	Substrate saturation current	24
15	Reverse current gain	24
16	Reverse Gummel plot	26
17	Output characteristics	28
18	Cut-off frequency $fT$	31
19	Temperature parameters	36
20	Summary	38

## Distribution



# 1 History of documentation

December 1996 : release of MEXTRAM parameter extraction report.

## 2 Introduction

The Philips state of the art MEXTRAM bipolar transistor model [1] has been put in the public domain in January 1994. It is suitable for digital and analog circuitry design and has demonstrated accuracy in a wide variety of applications. The accuracy of these circuit simulations not only depends on a correct mathematical description of several physical phenomena like current gain, output conductance, base push-out, cut-off frequency, noise behavior and temperature scaling but also on a reliable, robust and unambiguous transistor parameter extraction method. The use of a very sophisticated model with poorly determined parameters will result in a bad prediction of circuit performance. The definition of the transistor parameters is an important task in the development of a transistor model. A strong correlation between transistor parameters hampers unambiguous determination of individual parameters. Most parameters of the MEXTRAM model can be extracted directly from measured data. Therefore we need depletion capacitance ( $C_V$ ), terminal voltages versus currents (DC Gummel plots) and cut-off frequency ( $f_T$ ) measurements. To determine the parameters of the temperature scaling rules part of the measurements have to be repeated at another temperature.

In this document the minimum data needed to extract MEXTRAM transistor parameters is treated. Of course additional measurements (e.g. small signal Y parameters) can be carried out and used in the parameter extraction method.

To extract MEXTRAM transistor parameters the model is implemented in the IC-CAP program of Hewlett Packard. The complete MEXTRAM model is built into the MNS circuit simulator of HP and can also be used to extract transistor parameters or to verify simulated and measured data not used during parameter extraction. The MEXTRAM model is also able to evaluate vertical PNP transistors. In the next sections first the measurements to be carried out are described. Then the computation of the initial parameter set and the parameter extraction strategy are explained. The different steps in the parameter extraction and the used simplified MEXTRAM relations involved are described.

## 3 Measurements

To extract reliable parameters it is important that the measurements are done over a large range of collector, base and emitter biasing conditions. The number of data points in an interval is of minor importance. The maximum collector, base and emitter voltage are obtained from DC measurements. Therefore and also to avoid charge storage during the capacitance measurements, it is recommended to start with the DC measurements (see table 1). The first column gives the name assigned to the measurement setup (Measurement code: Mc).

Mc	Bias setting	Measured data
Veaf	f( $V_{cb} = 0 \dots V_{cb_{max}}$ ), $V_{be} = 0.65V$	$I_c, I_b$
Vear	f( $V_{eb} = 0 \dots V_{eb_{max}}$ ), $V_{bc} = 0.65V$	$I_e, I_b$
Forward	f( $V_{be} = 0.4 \dots 1.2$ ), $V_{bc} = 0.0V$	$I_c, I_b, I_{sub}$
Reverse	f( $V_{bc} = 0.4 \dots 1.2$ ), $V_{be} = 0.0V$	$I_e, I_b, I_{sub}$
IcVce	f( $V_{ce} = 0 \dots V_{cb_{max}} + 1$ ), $\frac{1}{4} \cdot I_{b3}$ , $\frac{1}{2} \cdot I_{b3}$ , $I_{b3}$	$V_{be}, I_c, I_{sub}$
Re	f( $V_{be} = 1.0 \dots 1.5$ ), $I_c < 1\mu A$	$V_{ce}, I_e$
Cbe	f( $V_{be} = -V_{eb_{max}} \dots 0.4$ )	$C_{be}$
Cbc	f( $V_{bc} = -V_{cb_{max}} \dots 0.4$ )	$C_{bc}$
Csc	f( $V_{sc} = -V_{cb_{max}} \dots 0.4$ )	$C_{sc}$
fT	f( $V_{be} = 0.75 \dots V_{be_{Ib3}}$ ), $V_{bc1} = 0.3$ , $V_{bc2}$ , $V_{bc3}$	$fT, I_c$

Table 1: Overview of the measurements.

The substrate voltage is normally set to  $-1$  Volt with respect to the common in the different measurement setups.

- The maximum collector voltage  $V_{cb_{max}}$  is obtained from the Early forward measurement and is the voltage where the base current becomes negative. This collector voltage is about the  $BV_{CEO}$  voltage (Breakdown- Voltage-Collector-Emitter-Open). The  $BV_{CEO}$  voltage is strongly process dependent and varies from 3 Volt battery supply up to 50 Volt for automotive applications. The maximum collector voltage is used in the measurement setup of the output characteristic  $I_c V_{ce}$  and the depletion capacitance  $C_{bc}$  measurement.
- The maximum reverse emitter voltage  $V_{eb_{max}}$  may be obtained from the reverse Early measurement setup. In this setup the base current should be more or less constant. The base current decreases due to the generation of avalanche and/or tunneling currents in the reversed biased b-e junction. Note that these currents are not described in the MEXTRAM model. The maximum reverse emitter voltage is normally much lower than the maximum collector voltage due to the high doping concentrations in the base and emitter regions. For advanced bipolar transistors the reverse base-emitter voltage may be lower than  $\approx 0.5V$  to avoid tunneling and avalanche currents. Then the  $V_{eb}$  range may be enlarged by biasing the b-e junction slightly in the forward mode ( $V_{eb} > -0.3V$ ).  
The maximum emitter-base voltage is used in the measurement setup of the depletion capacitance  $C_{be}$ .
- In the next step the forward and reverse Gummel plot are measured. The forward junction voltage varies from about  $0.4V$  up to  $1.2V$ . The reverse junction voltage is 0 Volt to avoid the generation of avalanche/tunneling currents and self-heating.
- Then the output characteristic is measured at three constant values of the base current. The value of the third base current ( $I_{b3}$ ) may be obtained from the



forward Gummel plot where the current gain is about the half of the maximum gain ( $V_{be} \approx 0.8V$ ). The value of the first base current is  $I_{b1} = \frac{1}{4} \cdot I_{b3}$  and the second base current becomes  $I_{b2} = \frac{1}{2} \cdot I_{b3}$ . The maximum collector voltage should be about  $BV_{CEO}$  out of the Early forward measurement setup plus 1 Volt. In this way the output characteristic normally exhibit sufficient quasi-saturation and/or high injection effect to extract the epilayer parameters and the knee current  $IK$ .

- In the Re measurement setup the transistor is biased in strong saturation to obtain the emitter resistance. The collector current is kept small  $< 1\mu A$  and the applied base-emitter voltage is swept from about 1 Volt up to 1.5 Volt. The measured emitter current is plotted versus the measured collector voltage. The slope at high emitter current (about  $2mA/\mu m^2$  emitter area) should be more or less constant and be the emitter resistance.
- Next the AC measurements are done. First the depletion capacitances are measured. The maximum reverse collector and emitter voltages are obtained from the forward and reverse Early measurement setup as explained previously. The maximum substrate-collector voltage may be taken equal to the maximum collector-base voltage. The maximum forward junction voltage is usually taken 0.4 Volt.
- Finally the cut-off frequency  $fT$  is measured. In this measurement the cut-off frequency  $fT$  is obtained from S-parameter measurements in the common emitter configuration. We measure  $fT$  at 3 constant DC values of  $V_{bc}$  as a function of the base-emitter voltage  $V_{be}$ . The maximum  $V_{be}$  should be about the  $V_{be}$  of the third curve in the output characteristic  $I_c V_{ce}$ . The lowest  $V_{cb}$  is  $-300mV$  (base-collector junction voltage is forward biased) and the highest  $V_{cb}$  depends on the maximum supply voltage (3, 5 or 12 Volt). The second  $V_{cb}$  is taken in between (range -0.3, 1, 3 Volt, -0.3, 2, 5 Volt or -0.3, 3, 12 Volt) At the maximum  $V_{be}$  the collector current has to be the same as the collector current level in the output characteristic ( $I_c V_{ce}$ ).

## 4 Initial parameter set

The first step in the extraction of model parameters is to generate an initial parameter set. An accurate calculation of the epilayer related parameters prevents a lot of troubles and improves the convergency. The epilayer parameters can be calculated when we know the emitter dimensions, the thickness and doping level of the epilayer. It is not possible to extract all the MEXTRAM model parameters from one measured transistor. For example  $XC_{JE}$  and  $XIBI$  are determined from geometrical scaling rules. Also the built-in field  $ETA$  of the active base is difficult to determine from electrical measurements. In practice for a certain process a constant value is taken depending on the doping profile of the base. Typical values are between 3 for low frequency  $fT < 1GHz$  and 6 for high frequency transistors  $fT > 20GHz$ . In

tables 2 and 3 for each parameter typical values are given. These are rounded values of the parameter list given in [1] to simulate the test data. The emitter dimensions are  $2 \times 6 \mu m$ . The epilayer thickness after processing is about  $0.8 \mu m$  and the doping level is about  $3 \cdot 10^{15}$ . Also the minimum and maximum parameter values are given to avoid numerical problems in the MEXTRAM model evaluation routines.

Parameter	Typical	$P_{min}$	$P_{max}$	remarks
<i>LEVEL</i>	503.2	—	—	
<i>EXMOD</i>	1	0	1	flag
<i>EXAVL</i>	0	0	1	flag
<i>IS</i>	$1 \cdot 10^{-17}$	$> 0$	—	scales with $A_e$
<i>BF</i>	150	$> 0$	—	
<i>XIBI</i>	0.0	$\geq 0$	$< 1$	
<i>IBF</i>	$1 \cdot 10^{-14}$	$\geq 0$	—	scales with $A_e$
<i>VLF</i>	0.5	$\geq 0$	—	
<i>IK</i>	$15 \cdot 10^{-3}$	eqn. 48	—	scales with $A_e$
<i>BRI</i>	5	$> 0$	—	
<i>IBR</i>	$1 \cdot 10^{-14}$	$\geq 0$	—	scales with $A_e$
<i>VLR</i>	0.5	$\geq 0$	—	
<i>XEXT</i>	0.5	$\geq 0$	$< 1$	
<i>QBO</i>	$1 \cdot 10^{-13}$	$> 0$	—	eqn. 8
<i>ETA</i>	4	$\geq 0$	$< 8$	
<i>AVL</i>	60	$> 0$	—	eqn. 6
<i>SFH</i>	0.3	$\geq 0$	—	eqn. 5
<i>EFI</i>	0.8	$> 0$	$\leq 1$	eqn. 7
<i>IHC</i>	$5 \cdot 10^{-4}$	$> 0$	—	eqn. 1
<i>RCC</i>	20	$> 0$	—	
<i>RCV</i>	1000	$> 0$	—	eqn. 2
<i>SCRCV</i>	2000	$> 0$	—	eqn. 3
<i>RBC</i>	100	$> 0$	—	scales with $1/A_e$
<i>RBV</i>	300	$> 0$	—	scales with $1/A_e$
<i>RE</i>	2	$> 0$	—	scales with $1/A_e$

Table 2: Typical, minimum and maximum parameter values.

Parameter	Typical	$P_{min}$	$P_{max}$	remarks
<i>TAUNE</i>	$5 \cdot 10^{-12}$	$\geq 0$	–	eqn. 11
<i>MTAU</i>	1	$\geq 1$	$\leq 2$	
<i>CJE</i>	$5 \cdot 10^{-14}$	$\geq 0$	–	scales with $A_e$
<i>VDE</i>	0.9	$> 0$	–	
<i>PE</i>	0.5	$> 0$	$< 1$	
<i>XCJE</i>	0.2	$\geq 0$	$< 1$	eqn. 13
<i>CJC</i>	$5 \cdot 10^{-14}$	$\geq 0$	–	scales with $A_c$
<i>VDC</i>	0.65	$> 0$	–	eqn. 4
<i>PC</i>	0.5	$> 0$	$< 1$	
<i>XP</i>	0.3	$> 0$	$< 1$	eqn. 10
<i>MC</i>	0.3	$\geq 0$	$\leq 0.5$	
<i>XCJC</i>	0.05	$> 0$	$< 1$	eqn. 9
<i>ISS</i>	$5 \cdot 10^{-17}$	$\geq 0$	–	scales with $A_c$
<i>IKS</i>	$5 \cdot 10^{-6}$	$> 0$	–	scales with $A_c$
<i>CJS</i>	$2 \cdot 10^{-13}$	$\geq 0$	–	scales with $A_c$
<i>VDS</i>	0.5	$> 0$	–	
<i>PS</i>	0.3	$> 0$	$< 1$	
<i>VGS</i>	1.12	–	$\leq 1.206$	
<i>AS</i>	1.9	$\geq 0$	2.3	
<i>TREF</i>	25	–	–	
<i>VGE</i>	1.13	–	$\leq 1.206$	
<i>VGB</i>	1.206	–	$\leq 1.206$	
<i>VGC</i>	1.13	–	$\leq 1.206$	
<i>VGJ</i>	1.13	–	$\leq 1.206$	
<i>VI</i>	$20 \cdot 10^{-3}$	–	–	
<i>NA</i>	$5 \cdot 10^{17}$	$> 10^{15}$	$< 10^{21}$	
<i>ER</i>	$2 \cdot 10^{-3}$	–	–	
<i>AB</i>	1.0	$\geq 0$	2.3	
<i>AEPI</i>	1.9	$\geq 0$	2.3	
<i>AEX</i>	0.3	$\geq 0$	2.3	
<i>AC</i>	0.26	$\geq 0$	2.3	
<i>KF</i>	$2 \cdot 10^{-11}$	$\geq 0$	–	scales with $1/A_e$
<i>KFN</i>	$5 \cdot 10^{-6}$	$\geq 0$	–	scales with $1/A_e$
<i>AF</i>	2.	–	–	
<i>DTA</i>	0	–	–	
<i>MULT</i>	1.	$> 0$	–	

Table 3: Typical, minimum and maximum parameter values.

The epilayer model parameters are,

$$IHC = q \cdot N_{epi} \cdot A_e \cdot v_{lim} \cdot \frac{1 + SFH}{\alpha_{cf}} \quad (1)$$

$$RCV = \frac{W_{epi}}{q \cdot N_{epi} \cdot \mu \cdot A_e} \cdot \frac{\alpha_{cf}}{1 + SFH} \quad (2)$$

$$SCRCV = \frac{W_{epi}^2}{2 \cdot \epsilon \cdot v_{lim} \cdot A_e} \cdot \frac{\alpha_{cf}}{1 + SFH} \quad (3)$$

$$VDC = V_t \cdot \ln \left\{ (N_{epi}/n_i)^2 \right\} \quad (4)$$

$$SFH = 2/3 \cdot \tan(\alpha_h) \cdot W_{epi} \cdot \left( \frac{1}{H_e} + \frac{1}{L_e} \right) \quad (5)$$

where

$$A_e = H_e \cdot L_e$$

$$SFH = \tan(\alpha_l) \cdot W_{epi} \cdot \left( \frac{1}{H_e} + \frac{1}{L_e} \right)$$

$$n_i^2 = 9.61 \cdot 10^{32} \cdot T^3 \cdot \exp\left(-\frac{VGC}{V_t}\right)$$

$$\mu = \mu_{min} + \frac{\mu_{max} - \mu_{min}}{1 + (N_{epi}/N_{ref})^\alpha}$$

$$\mu_{max} = 1360$$

$$\mu_{min} = 92$$

$$N_{ref} = 1.3 \cdot 10^{17}$$

$$\alpha = 0.91$$

$$q = 1.602 \cdot 10^{-19}$$

$$v_{lim} = 8 \cdot 10^6$$

$$\epsilon = 1.036 \cdot 10^{-12}$$

and  $\alpha_l$  is the spreading angle at low current levels ( $I_c < IHC$ ),  $\alpha_h$  the spreading angle at high current levels ( $I_c > IHC$ ),  $\alpha_{cf}$  the fraction of  $I_c$  flowing through the floor area of the emitter and  $L_e$  is the length of the emitter stripe, respectively. Typical values used in the calculations are,

$$\tan(\alpha_l) = 0.5$$

$$\tan(\alpha_h) = 1.0$$

$$\alpha_{cf} = 0.8$$

The avalanche parameter are,

$$AVL = B \cdot \sqrt{\frac{2 \cdot \epsilon \cdot VDC}{q \cdot N_{epi}}} \quad (6)$$

$$EFI = 2 \cdot \frac{1 + 2 \cdot SFH}{1 + 2 \cdot SFH} \cdot \frac{2 + SFH + 2 \cdot SFH}{2 + 3 \cdot SFH} - 1 \quad (7)$$

$$NPN: \quad B = 1.23 \cdot 10^6$$

$$PNP: \quad B = 2.04 \cdot 10^6$$

The initial value of the base charge  $QBO$  can be calculated from the value  $I_{e0}$  and the slope  $\Delta V_{be}/\Delta I_e$  at  $V_{be} = 0V$  of the emitter current of the reverse Early measurement;

$$QBO = I_{e0} \cdot (1 - XCJE) \cdot CJE \cdot \frac{\Delta V_{be}}{\Delta I_e} \quad (8)$$

An initial value for the parameters  $XCJC$ ,  $XP$  and  $TAUNE$  can be obtained in this way;

$$Xd_0 = \sqrt{\frac{2 \cdot \epsilon \cdot V_{dc}}{q \cdot N_{epi}}} \quad (9)$$

$$XCJC = \frac{H_e \cdot L_e \cdot \epsilon}{Xd_0 \cdot CJC} \quad (9)$$

$$XP = \frac{Xd_0}{W_{epi}} \quad (10)$$

$$TAUNE = \frac{1}{20 \cdot \max(fT)} \quad (11)$$

## 5 Parameter extraction strategy

The general strategy is to put the parameters in small groups (typical 1-3) and extract these parameters simultaneously out of measured data sensitive to these parameters. The composition of each individual group depends on the technology, however, it is possible to give general guide lines. A typical grouping of MEXTRAM parameters is given in table 4. The parameters have to be extracted in the sequence given in the table.

Mc	parameter(s)	input	output
Cbe	<i>CJE, VDE, PE</i>	Vbe	Cbe
Cbc	<i>CJC, XP, PC</i>	Vcb	Cbc
Csc	<i>CJS, VDS, PS</i>	Vsc	Csc
Vear	<i>QB0</i>	Veb, Vcb	Ie
Veaf	<i>XCJC</i>	Vcb, Veb	Ic
Veaf	<i>AVL</i>	Vcb, Veb, Ic	Ib
Re	<i>RE</i>	Vce, Ie	Re
Forward	<i>IS</i>	Veb, Vcb	Ic
Forward	<i>BF, VLF, IBF</i>	Veb, Vcb, Ic	Hfe
Forward	<i>RBC, RBV</i>	Vcb, Ic, Ib	Vbe
Reverse	<i>ISS</i>	Vcb, Veb	Hfc-sub
Reverse	<i>BRI, VLR, IBR</i>	Vcb, Veb	Hfc
Reverse	<i>IKS, RCC, XEXT</i>	Vcb, Veb, Ie	Ie, Ib, Is
IcVce	<i>RCV, IK, SCRCV</i>	Vce, Vbe, Ib	Ic
fT	<i>TAUNE, MTAU</i>	Vbe, Vce, Ic	fT

Table 4: Overview of the MEXTRAM parameter extraction.

The first column gives the name assigned to the measurement setup (measurement code). The column "parameter(s)" gives the MEXTRAM parameters to be extracted from the selected measurement code. The column "input" contains which values will be needed by the function for calculation of the quantity given in the last column, "output". The default reference temperature  $TREF$  for parameter determination is 25 °C. The temperature scaling rules of the parameters can be found on page 28, 29 and 30 of reference [1]. The MEXTRAM model is also able to evaluate vertical PNP transistors. Then the variable "type" in IC-CAP has to switch from NPN to PNP. For discrete NPN/PNP transistors the substrate saturation current  $ISS$  and the substrate capacitance  $CJS$  has to set to zero. The determination of  $RE$  is done by means of the open collector method (Giacolletto). The emitter resistance can be calculated directly from this measurement. The slope at high current level of  $I_e$  versus  $V_{ce}$  results into  $RE$  (current level : 2 mA/ $\mu m^2$  emitter area).

## 6 Equivalent electrical circuit

The electrical equivalent circuits for the vertical NPN transistor is shown in fig. 1

**Note:**

The elements in the figure indicates their position and NOT their functional dependence!

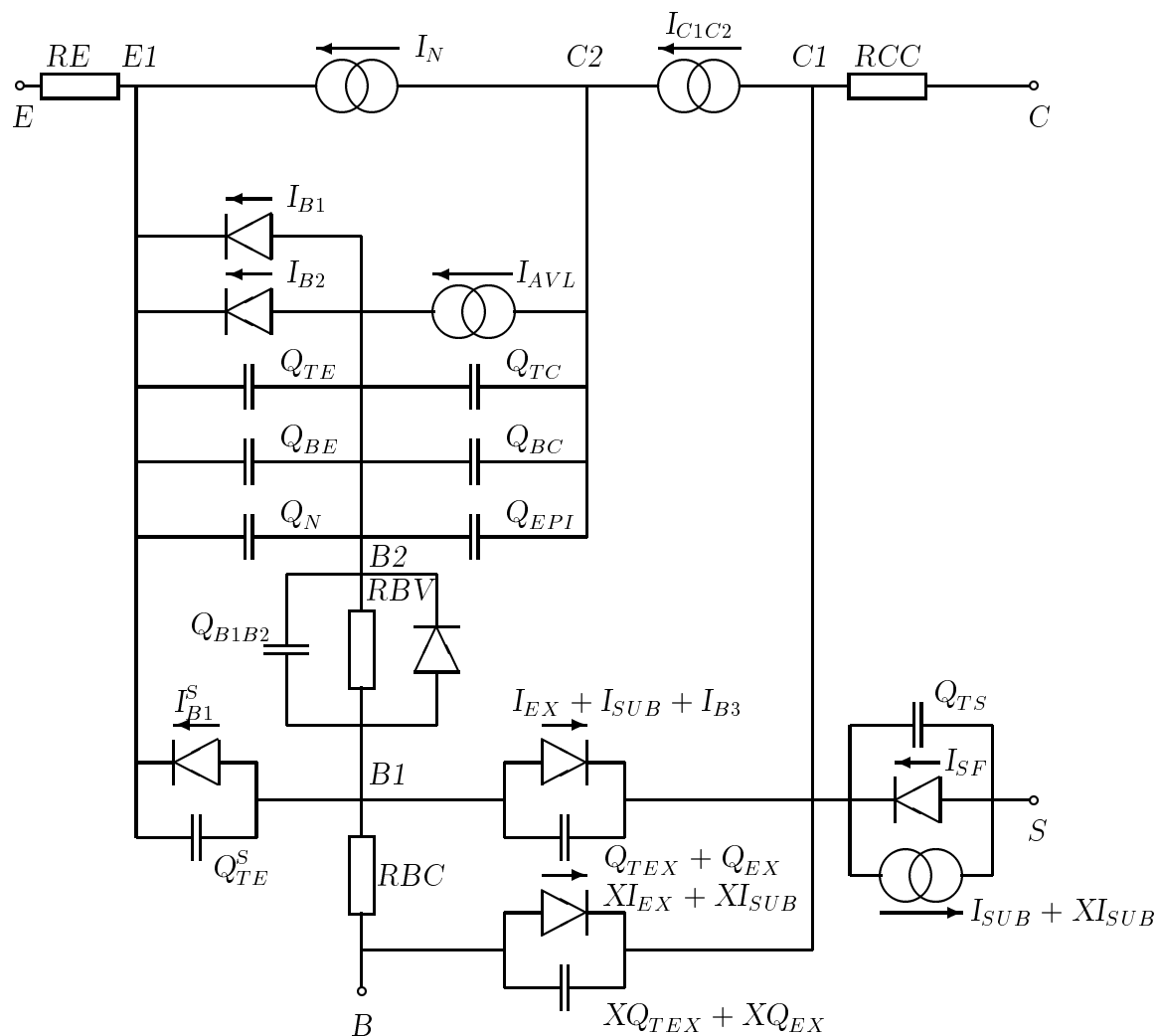


Figure 1: Equivalent circuit for vertical NPN transistor

## 7 Depletion Capacitances

- Base emitter depletion capacitance  $Cbe$

The formula for the base-emitter depletion capacitance is obtained from differentiating the charge  $Q_{TE}^{tot}$  (see [1] equation (2.73)) with respect to the base-emitter voltage  $Vbe$ :

$$Cbe = \frac{CJE_T \cdot (1 + K) \left( \frac{PE}{2} + 1 \right)}{(1 - PE + K) \cdot \left( \left( 1 - \frac{Vbe}{VDE_T} \right)^2 + K \right)^{\frac{PE}{2}}} \cdot \left[ 1 - \frac{PE \cdot \left( 1 - \frac{Vbe}{VDE_T} \right)^2}{\left( 1 - \frac{Vbe}{VDE_T} \right)^2 + K} \right] + CPBE \quad (12)$$

A constant parallel capacitance is  $CPBE$  is added to account for parasitic (envelope, bound pads etc.) capacitances. This capacitance is not included in the MEXTRAM model. An example of the base-emitter depletion capacitance parameter extraction is shown in figure 2. When the base-emitter depletion capacitance for transistors with different geometries is measured the parameter  $XCJE$  can be determined,

$$\begin{aligned} CJE &= CJE_b \cdot H_e \cdot L_e + 2 \cdot CJE_S \cdot (L_e + H_e) \\ XCJE &= \frac{2 \cdot CJE_S \cdot (L_e + H_e)}{CJE} \end{aligned} \quad (13)$$

where  $CJE_b$  and  $CJE_S$  are the capacitances per unit bottom area and sidewall length respectively. Note that the Early effect parameters  $QB0$  and  $XCJC$  scales with  $(1 - XCJE)$ . Therefore the scaling of the base-emitter depletion capacitance has to be done before doing the other extractions.

Input function	:	$V_{BE}$
Output function	:	$Cbe$
Extracted parameters	:	$CJE$ , $VDE$ , $PE$ , $CPBE$ , $(XCJE)$

- Base- collector depletion capacitance  $Cbc$

The total base-collector depletion capacitance is the sum of the charges  $Qtc$ ,  $Qtex$  and  $XQtex$  (see reference [1] equations (2.76 with  $ICAP = 0$ , 2.82 and 2.83 respectively). In all the equations the internal junction voltage is replaced by the terminal



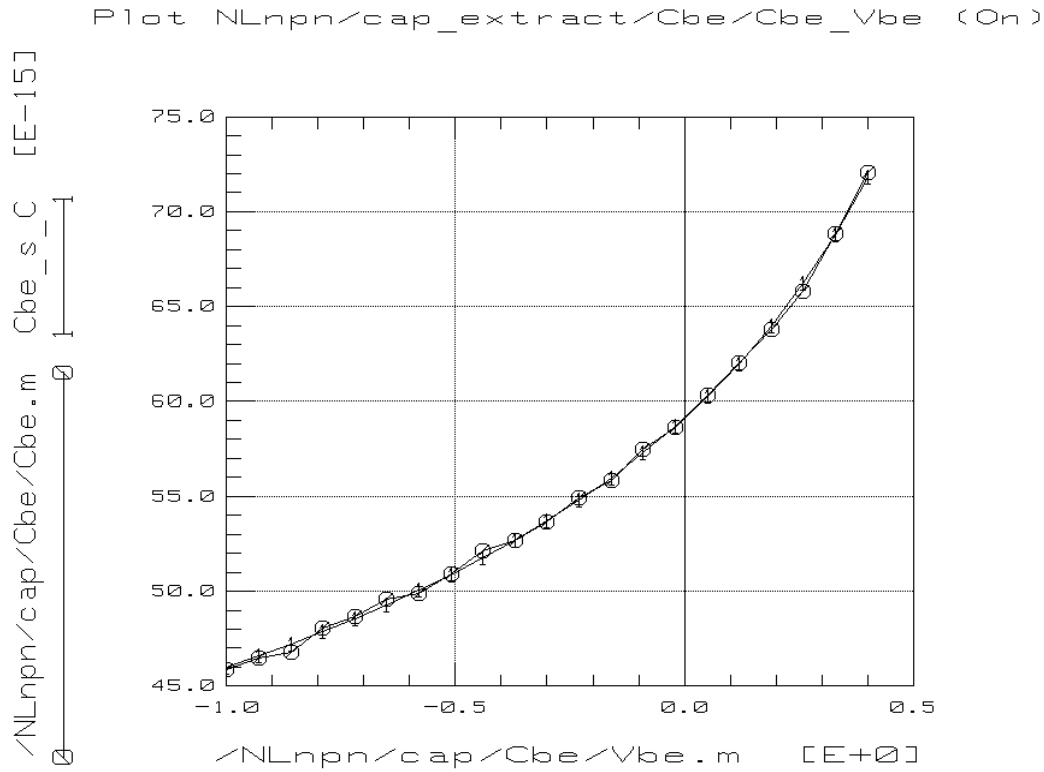


Figure 2: Measured and simulated base-emitter depletion capacitance. The extracted parameters are:  $CJE = 59.1fF$ ,  $VDE = 944mV$  and  $PE = 0.343$ .

voltage  $Vbc$ . The derivative of the charges with respect to the voltage  $Vbc$  gives the capacitance  $Cbc$ ,

$$Cbc = \frac{(1 - XP_T) \cdot CJC_T \cdot (1 + CK) \left(\frac{PC}{2} + 1\right)}{(1 - PC + CK) \cdot \left(\left(1 + \frac{Vcb}{VDC_T}\right)^2 + CK\right) \frac{PC}{2}} \cdot \left[ 1 - \frac{PC \cdot \left(1 + \frac{Vcb}{VDC_T}\right)^2}{\left(1 + \frac{Vcb}{VDC_T}\right)^2 + CK} \right] + XP_T \cdot CJC_T + CPBC \quad (14)$$

In MEXTRAM the DC and AC characteristics in quasi-saturation are sensitive to the diffusion voltage  $VDC$  and therefore  $VDC$  is extracted from these characteristics (see section 17). For  $Cbc$  an accurately description is still possible with a fixed value of the diffusion voltage because the decrease of the base-collector capacitance with collector voltage is mainly given by  $XP$  and  $PC$ . Note that the parasitic capacitance  $CPBC$  and  $XP$  can not be extracted simultaneously. Capacitance  $CPBC$  is not included in the MEXTRAM model. An example of the base-collector depletion

capacitance parameter extraction is shown in figure 3.

Input function :  $V_{cb}$   
 Output function :  $C_{bc}$   
 Extracted parameters :  $C_{JC}$ ,  $PC$ ,  $XP$  or  $CPBC$

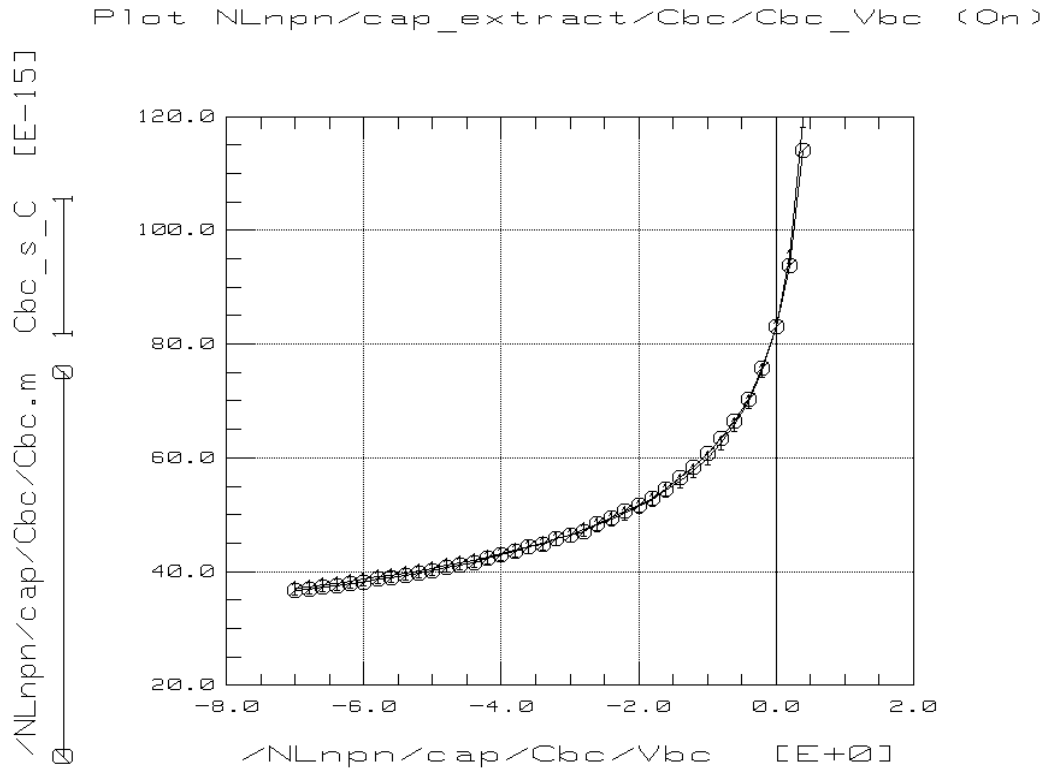


Figure 3: Measured and simulated base-collector depletion capacitance. The extracted parameters are:  $C_{JC} = 83.1\text{fF}$ ,  $PC = 0.371$  and  $XP = 0.100$ .

- Substrate-collector depletion capacitance  $C_{sc}$

The derivative of the charge  $Q_{ts}$  (see reference [1] equation 2.84) gives the depletion capacitance  $C_{sc}$ ,

$$C_{sc} = \frac{C_{JS_T} \cdot (1 + K) \left( \frac{PS}{2} + 1 \right)}{(1 - PS + K) \cdot \left( \left( 1 - \frac{V_{sc}}{V_{DS_T}} \right)^2 + K \right) \frac{PS}{2}}$$

$$\left[ 1 - \frac{PS \cdot \left(1 - \frac{V_{sc}}{V_{DS_T}}\right)^2}{\left(1 - \frac{V_{sc}}{V_{DS_T}}\right)^2 + K} \right] + CPCS \tag{15}$$

Note that the parameters *PS* and *CPCS* can not be extracted simultaneously. When *CPCS* has to be extracted then *PS* has to be fixed e.g. *PS* = 0.33. Capacitance *CPCS* is not included in the MEXTRAM model. For a discrete transistor the substrate-collector capacitance parameter *CJS* has to be set to zero. An example of the substrate-collector depletion capacitance parameter extraction is shown in figure 4.

Input function : *Vsc*  
 Output function : *Csc*  
 Extracted parameters : *CJS* , *VDS* , *PS* , *CPCS*

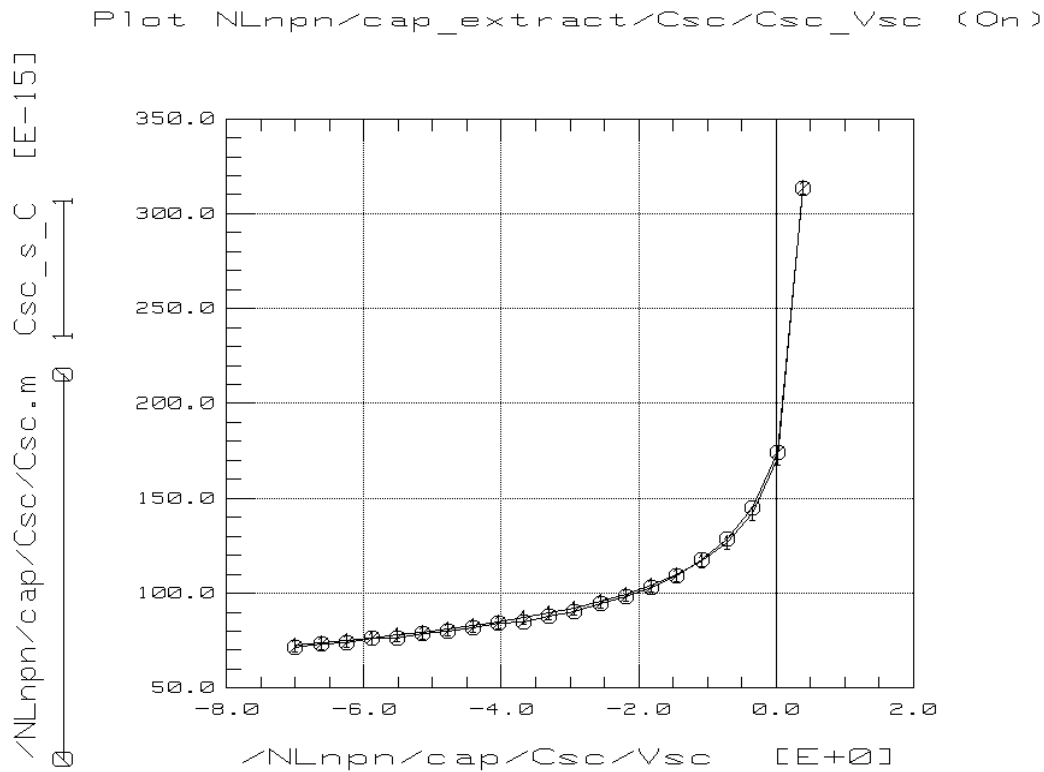


Figure 4: Measured and simulated substrate-collector depletion capacitance. The extracted parameters are: *CJS* = 167.6fF, *VDS* = 472mV and *PS* = 0.300.

## 8 Reverse Early effect

In this measurement setup the base-emitter junction voltage is varied and reverse biased and the base-collector junction is forward biased ( $V_{bc} \approx 0.65V$ ) and constant. In the MEXTRAM model the forward and reverse Early effect is bias dependent and is related to the depletion charges at the emitter-base and base-collector junction. The reverse Early voltage  $VAR$  can be calculated as follows;

$$VAR = \frac{1}{I_e} \cdot \frac{\partial I_e}{\partial V_{eb}} = \frac{C_{be}}{QB0_T + Q_{te} + Q_{tc}} \quad (16)$$

where  $C_{be}$  is the base-emitter depletion capacitance.

To calculate the depletion charges in this setup the internal junction voltages of the MEXTRAM model are replaced by the external applied voltages. In the formulation of  $Q_{tc}$  the current dependency may be neglected ( $I_{CAP} = 0$ ). Then the relation for  $Q_{tc}$  reduced to:

$$Q_{tc} = (1 - XP_T) \cdot XCJC \cdot \frac{CJC_T \cdot VDC_T \cdot (1 + CK)}{1 - PC + CK} \cdot \left[ 1 - \frac{\left(1 + \frac{V_{cb}}{VDC_T}\right) \cdot (1 + CK) \frac{PC}{2}}{\left(\left(1 + \frac{V_{cb}}{VDC_T}\right)^2 + CK\right) \frac{PC}{2}} \right] + XP_T \cdot CJC_T \cdot XCJC \cdot V_{cb} \quad (17)$$

The base-emitter depletion charge  $Q_{te}$  is;

$$Q_{te} = (1 - XCJE) \cdot \frac{CJE_T \cdot VDE_T \cdot (1 + K)}{1 - PE + K} \cdot \left[ 1 - \frac{\left(1 + \frac{V_{eb}}{VDE_T}\right) \cdot (1 + K) \frac{PE}{2}}{\left(\left(1 + \frac{V_{eb}}{VDE_T}\right)^2 + K\right) \frac{PE}{2}} \right] \quad (18)$$

The emitter current at zero bias ( $V_{be} = 0$ ) is  $I_{e0}$  and the increase of the emitter current with  $V_{be}$  becomes;

$$I_e = \frac{I_{e0}}{1 + \frac{Q_{te}}{QB0_T + Q_{tc}}} \quad (19)$$

The value of  $I_{e0}$  is extracted simultaneously with  $Q_{B0}$ . The parameter  $XCJC$  is extracted from the forward Early effect in the next step. Therefore the reverse and forward Early effect are extracted twice. The first time the initial value for  $XCJC$  is used. Normally  $Q_{tc}$  is small in comparison with  $Q_{B0}$  and one iteration is sufficient. An example of the reverse Early effect is shown in figure 5.

Input function :  $V_{eb}$  and  $V_{cb}$   
 Output function :  $I_e$   
 Extracted parameter :  $Q_{B0}$

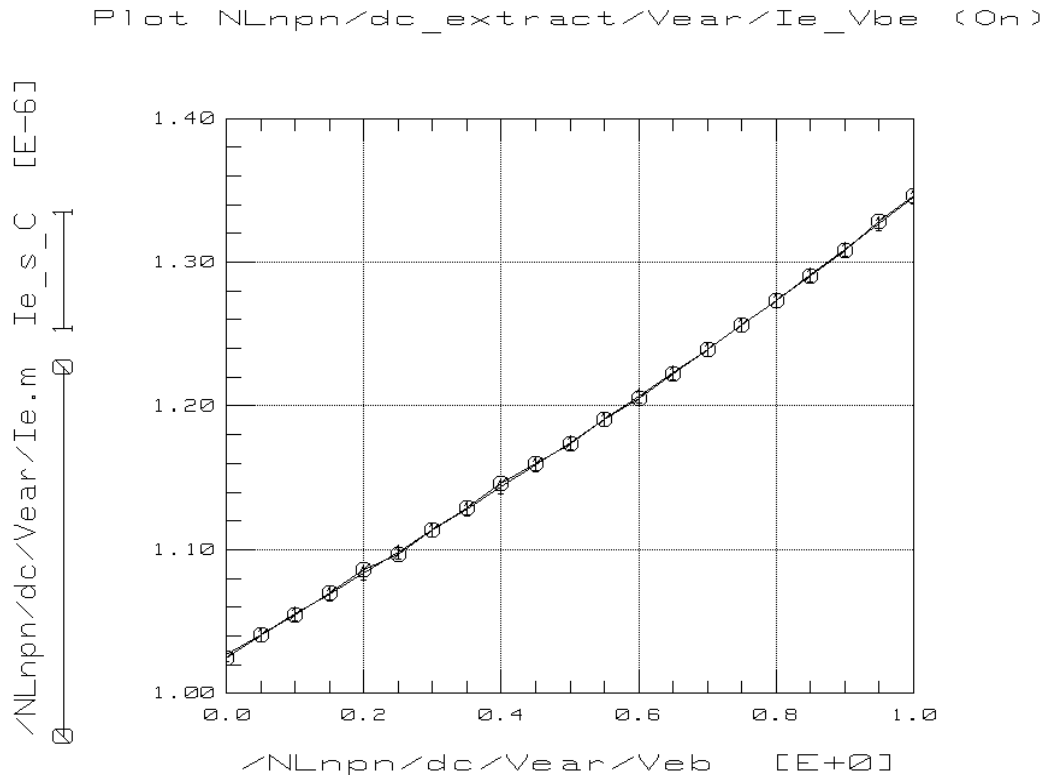


Figure 5: Measured and simulated reverse Early effect. The value of extracted parameter  $Q_{B0}$  is  $169.6fC$ .

## 9 Forward Early effect

In this measurement setup the collector–base junction voltage  $V_{cb}$  is varied and reverse biased and the base-emitter junction is forward biased ( $V_{be} \approx 0.65V$ ) and constant. This measurement setup is also used to extract the avalanche parameter  $AVL$ . From the measured data at small collector voltages the parameter  $XCJC$  is extracted to describe the increase of  $I_c$  with collector voltage. In this region the base current is constant. At higher values of  $V_{cb}$  the base current decreases due to the generation of avalanche current at the base–collector junction. At the

maximum applied collector voltage the base current have to be at least zero. This maximum collector voltage is strongly process dependent. It is important that the base–collector voltage range in the Early forward measurement and the the base–collector junction capacitance are the same. Because the width of the depletion layer obtained from the capacitance data determines also the bias dependency of the avalanche current. The forward Early effect is modeled in the same way as the reverse Early effect. The collector current at zero bias ( $V_{bc} = 0$ ) is  $I_{c0}$  and the increase of the collector current with  $V_{bc}$  becomes;

$$I_c = \frac{I_{c0}}{1 + \frac{Q_{tc}}{QB0_T + Q_{te}}} \quad (20)$$

The same equations (eqn. 17, 18) as defined for the Reverse Early effect are used to calculate the depletion charges  $Q_{te}$  and  $Q_{tc}$ . The value of  $I_{c0}$  is extracted simultaneously with  $XCJC$ . An example of the Early effect is shown in figure 6.

Input function :  $V_{eb}$  and  $V_{cb}$   
 Output function :  $I_c$   
 Extracted parameter :  $XCJC$

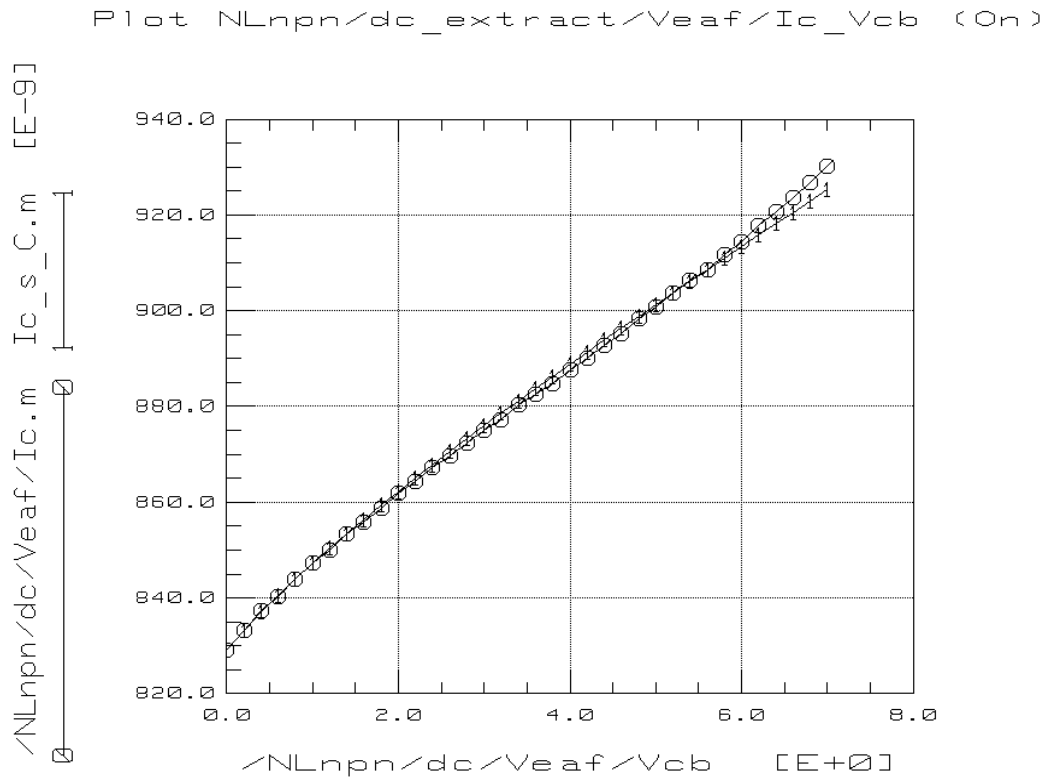


Figure 6: Measured and simulated forward Early effect. The parameter  $XCJC$  is extracted from the region where the base current is constant ( $0V < V_{cb} < 2V$ ). The extracted value of parameter  $XCJC$  is 0.064.

## 10 Avalanche

The avalanche effect and the forward Early effect are extracted from the same measurement setup. As shown in the previous section the Early effect is modeled from the increase of the collector current at small values of the collector voltage and now the avalanche effect is modeled from the decrease of the base current at high values of the collector voltage. At the maximum collector voltage the base current have to be at least zero. This collector voltage is about the *BVCEO* voltage (Breakdown-Voltage-Collector-Emitter-Open). An accurate modeling of the base-collector depletion capacitance *Cbc* up the *BVCEO* voltage is important because the width of the depletion layer is used to calculate the maximum electric field at the b-c junction. Therefore it is recommended to do the capacitance measurement also up to the *BVCEO* voltage.

The full avalanche model described in [1] reduced drastically when the collector current is sufficient small and does not modify the electric field distribution within the depletion layer ( $I_c/I_{HC} < 10^{-2}$ ). Then the reduced avalanche model becomes;

$$\begin{aligned}
 WD_{epi} &= \frac{AVL_T}{B_n \cdot XP_T} \\
 F_c &= \frac{1 - XP_T}{\left(1 + \frac{V_{cb}}{VDC_T}\right) PC} + XP_T \\
 W_d &= \frac{AVL_T}{F_c \cdot B_n} \\
 dEW_d &= \frac{VDC_T \cdot B_n}{F_c \cdot AVL_T} \\
 E_m &= \frac{V_{cb} \cdot VDC_T}{W_d + dEW_d} \\
 E_1 &= \frac{V_{cb} + VDC_T}{W_d} \\
 X_d &= \frac{E_m \cdot W_d}{2 \cdot (E_m - E_1)} \\
 G_{EM} &= \frac{A_n}{B_n} \cdot E_m \cdot W_d \cdot \left[ \exp\left(\frac{-B_n}{E_m}\right) - \exp\left(\frac{-B_n}{E_m} \cdot \left(1 + \frac{W_d}{X_d}\right)\right) \right] \quad (21)
 \end{aligned}$$

$$I_b = I_{b0} - I_c \cdot G_{EM} \quad (22)$$

where *Ib0* is the base current at small collector voltages. The values of *Ib0* and *AVL* are extracted simultaneously. An example of the avalanche effect is shown in figure 7.

Input function :  $V_{cb}$  and  $I_c$   
 Output function :  $I_b$   
 Assumptions :  $I_c/I_{HC} < 10^{-2}$   
 Extracted parameter :  $AVL$

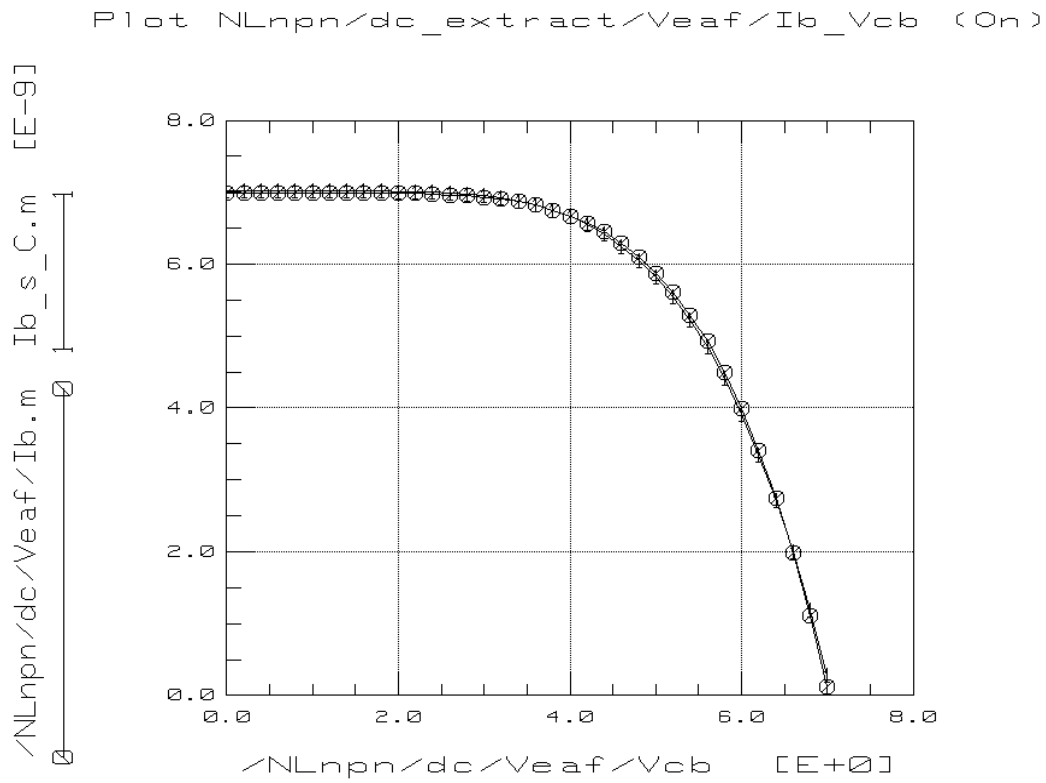


Figure 7: Measured and simulated decrease of the base current due to the avalanche effect. The value of extracted parameter  $AVL$  is 37.3.



## 11 Collector saturation current

In the Gummel plot the collector, base and substrate current are measured as a function of the base-emitter voltage at constant base-collector voltage. The base-collector voltage in the Gummel plot should be small ( $V_{bc} \approx 0$ ) to avoid self heating at high current level and to avoid the generation of avalanche currents. The collector saturation current  $IS$  is extracted from the Gummel plot at small values of the base-emitter voltage ( $0.4 < V_{be} < 0.65$ ). At these small  $V_{be}$  values high injection, saturation and series resistances effects may be neglected. The saturation current has to be corrected for the forward and reverse Early effect. The simplified expression for the collector current becomes:

$$I_c = \frac{IS_T \cdot \left( \exp\left(\frac{V_{be}}{V_T}\right) - 1 \right)}{1 + \frac{Q_{te} + Q_{tc}}{QB0_T}} \quad (23)$$

where  $V_T$  is the thermal voltage,  $Q_{tc}$  and  $Q_{te}$  are the base-emitter and base-collector depletion charges. They are defined by equations 17 and 18 respectively. An example of the extraction of the collector saturation current is shown in figure 8.

Input function	: $V_{eb}$ and $V_{cb}$
Output function	: $I_c$
Approximations	: $Q_{be} = 0, Q_{bc} = 0, I_r = 0, V_{b_2e_1} = -V_{eb}, V_{b_2c_2} = V_{bc}$
Extracted parameter	: $IS$

## 12 Forward current gain

The forward current gain parameters ( $ILF$ ,  $VLF$  and  $BF$ ) up to medium current levels are extracted from the forward Gummel plot. First from the measured collector current the internal base-emitter junction voltage  $V_{b_2e_1}$  is calculated. In this calculation high injection and saturation effects are neglected and as a consequence only measured data up to the roll off of the current gain ( $0.4V < V_{be} < 0.80...0.9V$ ) have to be selected in the optimization range. The depletion charges are calculated using the external applied voltages. This procedure eliminates the series resistance effect at medium current levels. The internal junction voltage becomes;

$$V_{b_2e_1} = V_T \cdot \ln \left( \frac{I_c \cdot \left( 1 + \frac{Q_{te} + Q_{tc}}{QB0_T} \right)}{IS_T} \right) \quad (24)$$

where  $V_T$  is the thermal voltage,  $Q_{tc}$  and  $Q_{te}$  are the base-emitter and base-collector depletion charges. They are defined by equations 17 and 18 respectively.

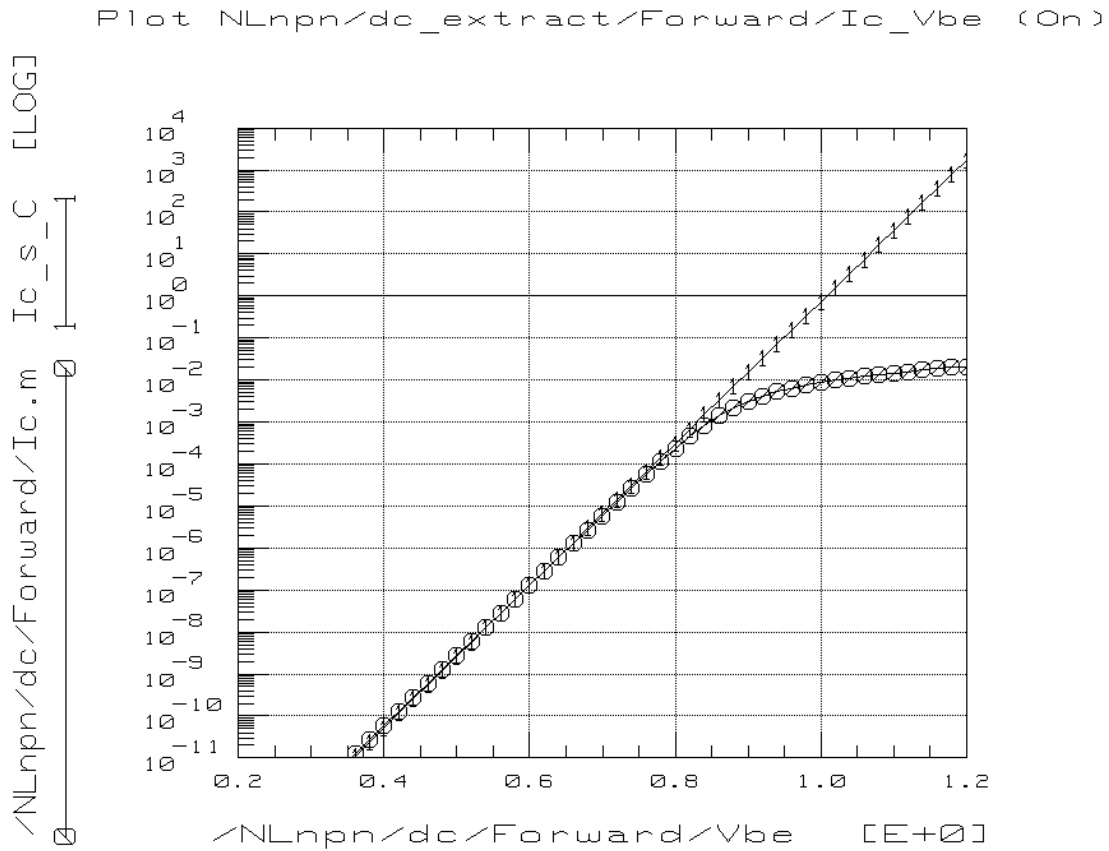


Figure 8: Measured and simulated collector current. The parameter  $IS$  is extracted from the collector current at small values of  $V_{be}$ . The value of the extracted parameter  $IS$  is 8.80 aA.

The ideal base current  $I_{b1}$  and the non-ideal base current  $I_{b2}$  are calculated using this  $V_{b2e1}$ ;

$$I_{b1} = \frac{IS_T}{BF_T} \cdot \left( \exp\left(\frac{V_{b2e1}}{V_T}\right) - 1 \right) \quad (25)$$

$$I_{b2} = IBF_T \cdot \frac{\exp\left(\frac{V_{b2e1}}{V_T}\right) - 1}{\exp\left(\frac{V_{b2e1}}{2 \cdot V_T}\right) + \exp\left(\frac{V_{LF_T}}{2 \cdot V_T}\right)} + G_{min} \cdot (V_{be} - V_{cb}) \quad (26)$$

The forward current gain  $HFE$  is,

$$HFE = \frac{I_c}{I_{b1} + I_{b2}} \quad (27)$$

An example of the measured and simulated current gain is shown in figure 9. Note that the roll-off of the gain due to high injection and/of quasi-saturation is not described.

Input function :  $V_{be}$ ,  $V_{cb}$  and  $I_c$   
 Output function :  $HFE$   
 Approximations :  $Q_{be} = 0$ ,  $Q_{bc} = 0$ ,  $I_r = 0$   
 Depletion charges :  $V_{b_2e_1} = V_{be}$  and  $V_{b_2c_2} = V_{bc}$   
 Extracted parameters :  $IBF$ ,  $VLF$  and  $BF$

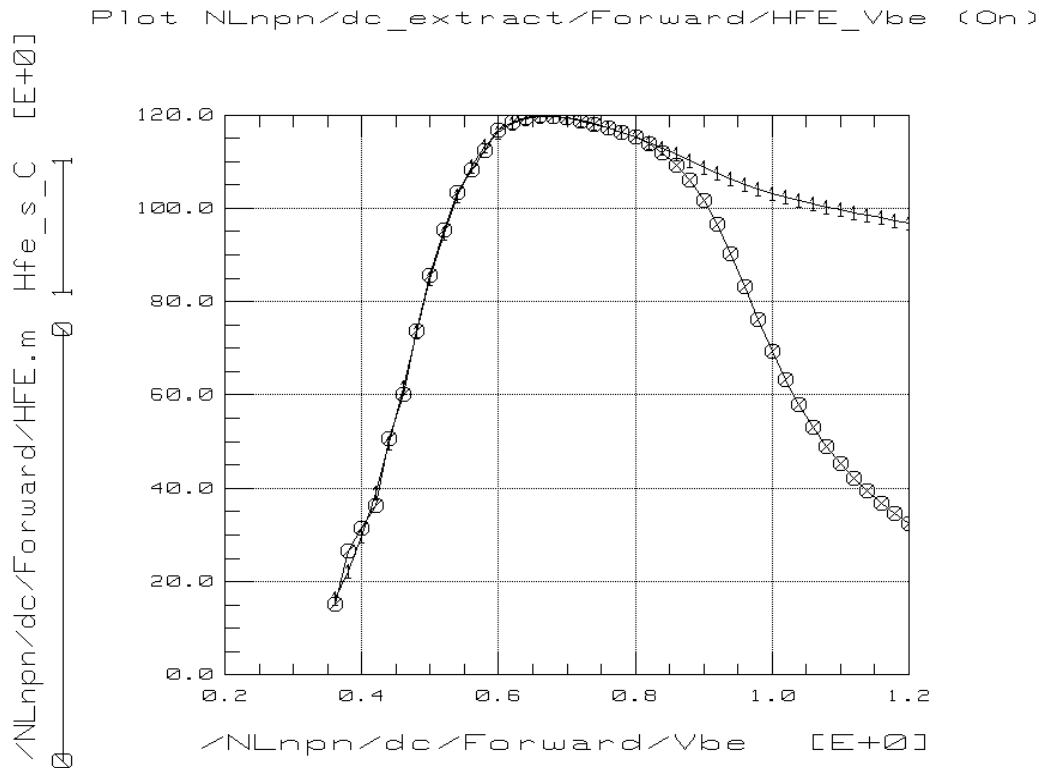


Figure 9: Measured and simulated forward current gain. The roll-off of the gain at high current levels is not described and these data points should therefore be excluded from the optimization range. The value of extracted parameters are:  $BF = 149.5$ ,  $IBF = 588\text{aA}$  and  $VLF = 258\text{mV}$ .

### 13 Base series resistances

The constant and variable part of the base series resistance may be obtained from the high current regime of the forward Gummel plot. However in practice it is very difficult to get a reliable value for the variable part  $RBV$  of the base resistance because the voltage drop is in many cases dominated by the constant part  $RBC$  and the emitter resistance  $RE$ . In particular the emitter resistance of poly-emitter devices may be high. My experience is that when we know the emitter dimensions, the sheet resistance of the pinched base, and the number of base contacts the value of  $RBV$  can be estimated fairly well by calculation.

The emitter series resistance is obtained from the open collector measurement setup (Giacoletto method) at high base voltages ( $V_{be} > 1.2\text{V}$ ). Then from the forward

Gummel plot only the constant part of the base resistance  $Rbc$  has to be extracted.

The external base–emitter voltage is:

$$Vbe = Vb_2e_1 + (Ic + Ib) \cdot RE + Ib \cdot (RBC_T + RBV'_T)$$

where  $RBV'_T$  is bias dependent due to charge modulation and current crowding effects. In the MEXTRAM model the charge modulation of  $RBV$  is given by;

$$Rbv_T = \frac{RBV_T}{1 + \frac{Qte + Qtc + Qbe + Qbc}{QBO}}$$

The charge modulation term is obtained from the description of the collector current;

$$Ic = \frac{If - Ir}{1 + \frac{Qte + Qtc + Qbe + Qbc + Qepi}{QBO}} \quad (28)$$

If we take care that the base–collector junction voltage  $Vb_2c_1$  is sufficient small ( $Vb_2c_1 < 0.4V$  'no hard saturation') and therefore  $Ir \approx 0$ , and we neglect the collector epilayer charge  $Qepi$  the charge modulation term of the base–resistance becomes;

$$Rbv_T = RBV_T \cdot \frac{Ic}{If} \quad (29)$$

Next we assume that at these high current level the base current is dominated by the ideal part;

$$Ib = \frac{IS_T}{BF_T} \cdot \left( \exp\left(\frac{Vb_2e_1}{V_t}\right) - 1 \right) = \frac{If}{BF_T} \quad (30)$$

From equation 30 we can calculate the internal base–emitter junction voltage  $Vb_2e_1$ . The DC current crowding of the pinched base is approximated in this way;

$$Vb_1b_2 = V_t \cdot \ln\left(1 + \frac{Rbv_T \cdot Ib}{V_t}\right) \quad (31)$$

After substitution of equations 29 and 30 in equation 31 the voltage drop of the variable part of the base resistance becomes;

$$Vb_1b_2 = V_t \cdot \ln\left(1 + \frac{RBV_T \cdot Ic}{BF_T \cdot V_t}\right) \quad (32)$$

The external base–emitter voltage now becomes;

$$Vbe = Vb_2e_1 + Vb_1b_2 + (Ic + Ib) \cdot RE + Ib \cdot RBC_T + Voff_{Rb} \quad (33)$$

In the above equation a small offset voltage  $V_{off_{Rb}}$  is added to correct for the difference between  $V_{be}$  and  $V_{b_2e_1}$  at medium values of the base current. This difference may be due to the presence of the non-ideal base current and the approximation of the bias dependency of the variable part of the base resistance. The internal junction voltage  $V_{b_2e_1}$  is calculated from equation 30. The model parameter  $RBC$  and the offset voltage  $V_{off_{Rb}}$  are extracted simultaneously. An example of the extraction of the constant part of the base resistance is shown in figure 10.

- Input functions :  $I_c$  and  $I_b$
- Output function :  $V_{be}$
- Parameters used :  $IS$ ,  $BF$ ,  $(RBV)$  and  $RE$
- Extracted parameter(s) :  $RBC$ ,  $(RBV)$
- Approximations : Charge modulation term  $Q_{epi} = 0$
- : Non-ideal base current neglected in the calculation of the internal b-e junction voltage.
- : First order DC current crowding.

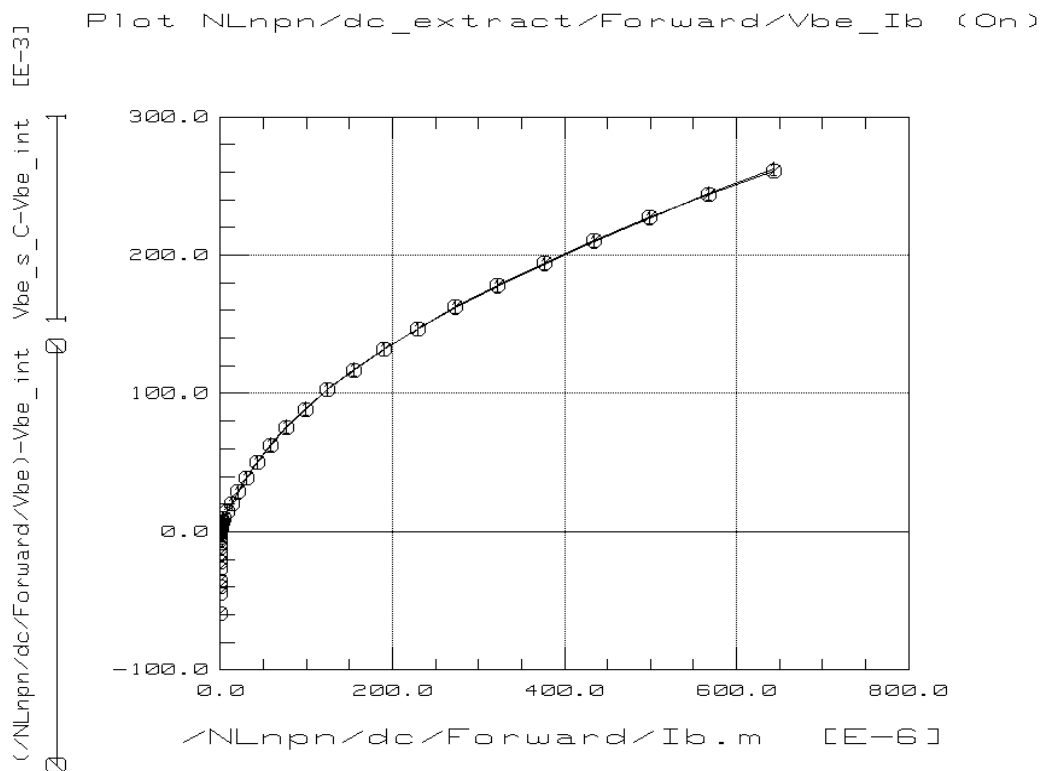


Figure 10: Measured and simulated voltage drop over the base and emitter resistance to extract parameter  $RBC$ . The value of  $RBC$  is  $50.9\Omega$ .

## 14 Substrate saturation current

The substrate saturation current  $ISS$  of the parasitic PNP transistor is obtained from the reverse Gummel plot. In this measurement setup the emitter, base and substrate current are measured as a function of the base–collector voltage at constant base–emitter voltage. In principal we can extract  $ISS$  directly from the substrate current at small values of  $Vbc$ ;

$$I_{sub} = ISS_T \cdot \left( \exp\left(\frac{Vbc}{V_T}\right) - 1 \right)$$

When a part of the base of the parasitic PNP has a small Gummel number the substrate current is large and dominates the reverse base current. Then under some circumstances we are not able to describe later on the reverse current gain. We can avoid this situation by extracting the substrate saturation current from the current gain of the parasitic PNP transistor;

$$HFC_{SUB} = \frac{I_e}{I_{sub}} \quad (34)$$

The emitter current of the reverse Gummel plot at small values of  $Vbc$  without high injection effects is;

$$I_e = \frac{IS_T \cdot \left( \exp\left(\frac{Vbc}{V_T}\right) - 1 \right)}{1 + \frac{Qte + Qtc}{QBO_T}}$$

Substitution of  $I_e$  and  $I_{sub}$  in (34) gives;

$$HFC_{SUB} = \frac{IS_T}{ISS_T \cdot \left( 1 + \frac{Qte + Qtc}{QBO_T} \right)} \quad (35)$$

where the depletion charges  $Qte$  and  $Qtc$  are defined by equations 18 and 17 respectively. An example of the current gain of the parasitic PNP is shown in figure 11.

Input function	:	$V_{eb}$ and $V_{cb}$
Output function	:	$HFC_{SUB}$
Extracted parameter	:	$ISS$
Approximations	:	No high injection effects in $I_e$ and $I_{sub}$

## 15 Reverse current gain

The reverse current gain parameters ( $IBR$ ,  $VLR$ ,  $BRI$  and  $IKS$ ) are extracted from the reverse Gummel plot. The proposed method is the same as for the forward

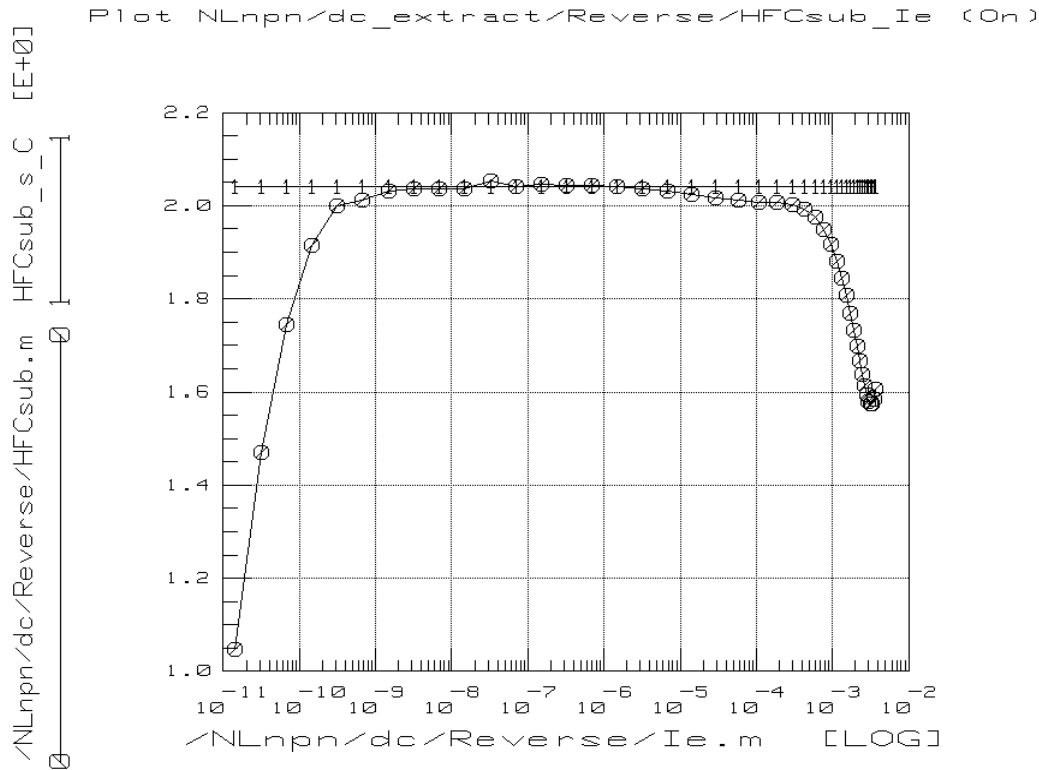


Figure 11: Measured and simulated current gain of the parasitic PNP transistor to extract the substrate saturation current. The extracted value of parameter  $ISS$  is  $3.89\mu A$ .

current gain. First from the measured emitter current the internal base–collector junction voltage  $V_{b_1c_1}$  is computed neglecting high injection as follows:

$$V_{b_1c_1} = V_T \cdot \ln \left( \frac{I_e \cdot \left( 1 + \frac{Q_{te} + Q_{tc}}{QB0_T} \right)}{IS_T} \right) \quad (36)$$

where  $V_T$  is the thermal voltage,  $Q_{tc}$  and  $Q_{te}$  are the base–emitter and base–collector depletion charges. They are defined by equations 17 and 18 respectively. The reverse base current consists of the substrate current, the ideal reverse base current and the non-ideal reverse base current. The substrate current, including high injection is,

$$I_{sub} = \frac{2 \cdot ISS_T \cdot \exp \left( \frac{V_{b_1c_1}}{V_T} - 1 \right)}{1 + \sqrt{1 + 4 \cdot \frac{IS_T}{IKS_T} \cdot \left( \exp \left( \frac{V_{b_1c_1}}{V_T} \right) - 1 \right)}} \quad (37)$$

The increase of the reverse current gain at medium current levels ( $I_e \approx 10\mu A$ ) is due to high injection effects in the substrate current. The substrate knee current is

small when the base (is the low doped epilayer) of the parasitic PNP transistor has a low Gummel number.

The non-ideal reverse base current (recombination in the b-c depletion layer) is,

$$I_{b3} = IBR_T \cdot \frac{\exp\left(\frac{V_{b_1c_1}}{V_T}\right) - 1}{\exp\left(\frac{V_{b_1c_1}}{2 \cdot V_T}\right) + \exp\left(\frac{V_{LR_T}}{2 \cdot V_T}\right)} + G_{min} \cdot (V_{bc} - V_{eb}) \quad (38)$$

The reverse base current  $I_{ex}$  of the NPN transistor without high injection ( $n_{b_{ex}} \ll 1$ , equation 2.45 [1]) is,

$$I_{ex} = \frac{IS_T}{BRI} \cdot \left( \exp\left(\frac{V_{b_1c_1}}{V_T}\right) - 1 \right) \quad (39)$$

Then the reverse current gain  $HFC$  becomes,

$$HFC = \frac{I_e}{I_{b3} + I_{sub} + I_{ex}} \quad (40)$$

An example of the reverse current gain is shown in figure 12.

Input function	:	$V_{eb}$ and $V_{cb}$
Output function	:	$HFC$
Extracted parameters	:	$BRI$ , $VLR$ , $IBR$ and $IKS$
Approximations	:	No high injection in $I_e$ and $I_{ex}$

## 16 Reverse Gummel plot

In this section the high currents,  $I_e$ ,  $I_b$ , and  $I_{sub}$ , of the reverse Gummel plot are described. The absolute value of the reverse currents are effected by the constant part of the collector resistance  $RCC$ , the constant part of the base resistance  $RBC$  and the partitioning of the extrinsic base-collector area over the branches  $b_1 - c_1$  and  $b - c_1$  (see figure 1). This partitioning is given by the parameter  $XEXT$ . Also the substrate knee current  $IKS$  can be extracted from these measurements. The currents to be calculated are a function of five internal junction voltages ( $V_{b_2c_2}$ ,  $V_{b_2c_1}$ ,  $V_{b_1c_1}$ ,  $V_{bc_1}$  and  $V_{b_2e_1}$ ). Starting with an initial guess for  $V_{b_2c_2}$  and an approximation for  $V_{b_2e_1}$  we can compute the other junction voltages including the terminal voltage  $V_{bc}$ . The difference with the applied  $V_{bc}$  set the new value of  $V_{b_2c_2}$  for the next iteration until convergency is reached ( $V_{bc}^n - V_{bc} < 10^{-4}V$ ), In this section we will refer to the formulae in [1] for the description of the different charge and current components.



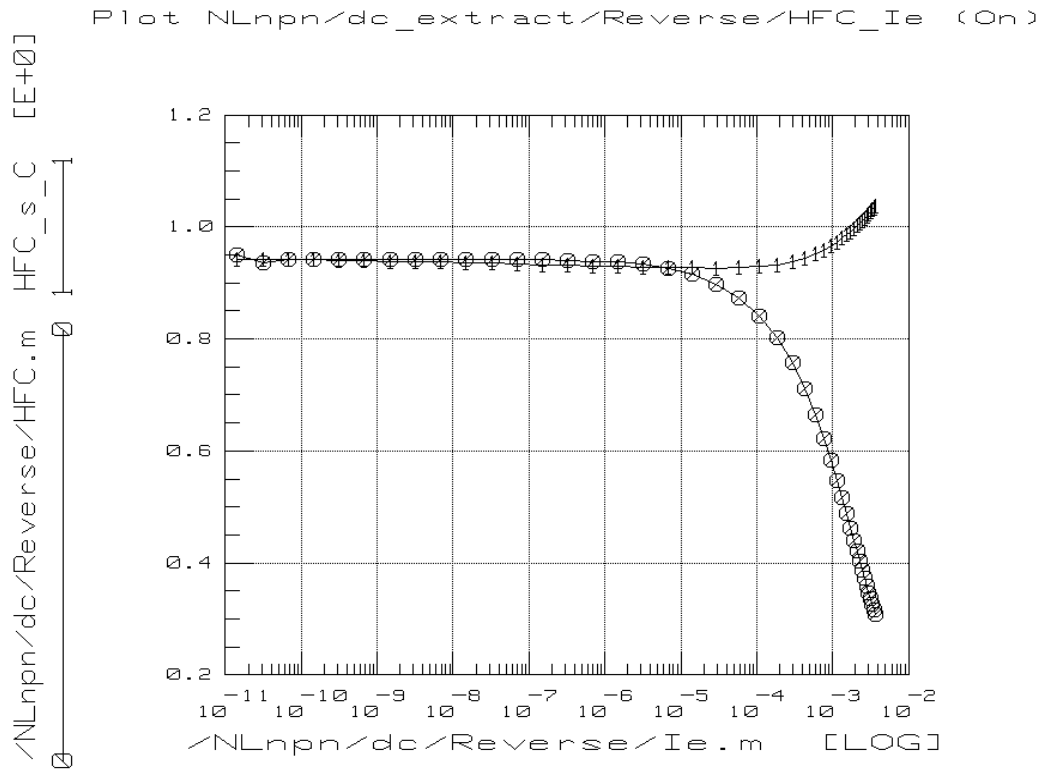


Figure 12: Measured and simulated reverse current gain. The value of extracted parameter  $BRI$  is 1.65.

The internal reverse junction voltage  $V_{b_2e_1}$  is,

$$V_{b_2e_1} = V_{be} + I_e \cdot RE - (I_{ex} + I_{sub}) \cdot RBC_T$$

where  $I_{ex}$ ,  $I_{sub}$  and  $I_e$  are taken from the previous iteration. The emitter current  $I_e$  is,

$$I_e = \frac{IS_T \cdot \left( \exp\left(\frac{V_{b_2c_2}}{V_T}\right) - 1 \right)}{1 + \frac{Q_{te} + Q_{tc} + Q_{bc}}{QBO_T}} \tag{41}$$

where from [1]  $Q_{te}$ ,  $Q_{tc}$  and  $Q_{bc}$  are given by equations 2.74, 2.76 with  $I_{CAP} = 0$  and 2.89 respectively. The junction voltage  $V_{b_2c_1}$  (voltage drop over the epilayer) is solved by applying the Kirchoff law to node  $c_2$ ;

$$I_n = I_{c_1c_2} = I_e$$

where  $I_{c_1c_2}$  is given by equation [1] 2.69. In the reverse mode of operation there is no voltage drop over the variable part of the base resistance because all reverse base-current components are positioned at the extrinsic base-collector junction and therefore  $V_{b_1c_1} = V_{b_2c_1}$ . Now we can calculate the currents  $I_{sub}$  ([1] eqn. 2.43)

and  $I_{ex}$  ([1] eqn. 2.45) of branch  $b_1 - c_1$ . In the extended reverse modeling mode  $EXMOD = 1$  these currents are multiplied with the factor  $(1 - XEXT)$  ([1] eqn. 2.101, 2.102). The junction voltage  $V_{bc_1}$  becomes,

$$V_{bc_1} = V_{b_1c_1} + (I_{ex} + I_{sub}) \cdot R_{BC_T}$$

The external base-collector voltage  $V_{bc}$  becomes:

$$V_{bc} = V_{bc_1} + (I_{ex} + XI_{ex} + I_e) \cdot R_{CC_T} \quad (42)$$

The computed  $V_{bc}$  has to be equal to the applied  $V_{bc}$ . This is achieved by an iterative solution of the voltage  $V_{b_2c_2}$ .

In the next step the currents  $XI_{sub}$  ([1] eqn. 2.110) and  $XI_{sub}$  [1] eqn. 2.111) are calculated depending on the  $EXMOD$  flag. The total substrate current  $I_{sub}$  and the reverse base current  $I_b$  becomes,

$$I_{sub} = -(I_{sub} + XI_{sub}) \quad (43)$$

$$I_b = I_{ex} + XI_{ex} + I_{sub} + XI_{sub} \quad (44)$$

An example of the modeling of the reverse Gummel plot is shown in figures 13 and 14.

Input function	: $V_{eb}$ and $V_{cb}$
Output function	: $I_e$ , $I_b$ and $I_{sub}$
Extracted parameter	: $XEXT$ , $RCC$ , ( $IKS$ )
Approximations	: $Q_{tc}$ with $I_{CAP} = 0$
	: Non-ideal base current $IB3$ neglected.

## 17 Output characteristics

In this setup we measure at three constant values of the base current the collector current  $I_c$ , the base-emitter voltage  $V_{be}$  and the substrate current  $I_{sub}$  as a function of the collector-emitter voltage  $V_{ce}$ . The base currents have to be sufficient high so that the collector current exhibit quasi-saturation and/or high injection effects. Preferable the largest collector current has to be up to 2-4 times the estimated value of the hot-carrier current  $I_{HC}$ . The region where a noticeable substrate current is present indicates the hard-saturation region of the transistor. Without self-heating of the device the base-emitter voltage  $V_{be}$  increases with the collector voltage ( $\Delta V_{be} = \Delta I_c \cdot RE$ ). In many cases self-heating influence the measured output characteristics significantly and  $V_{be}$  decreases with increasing  $I_c$ .

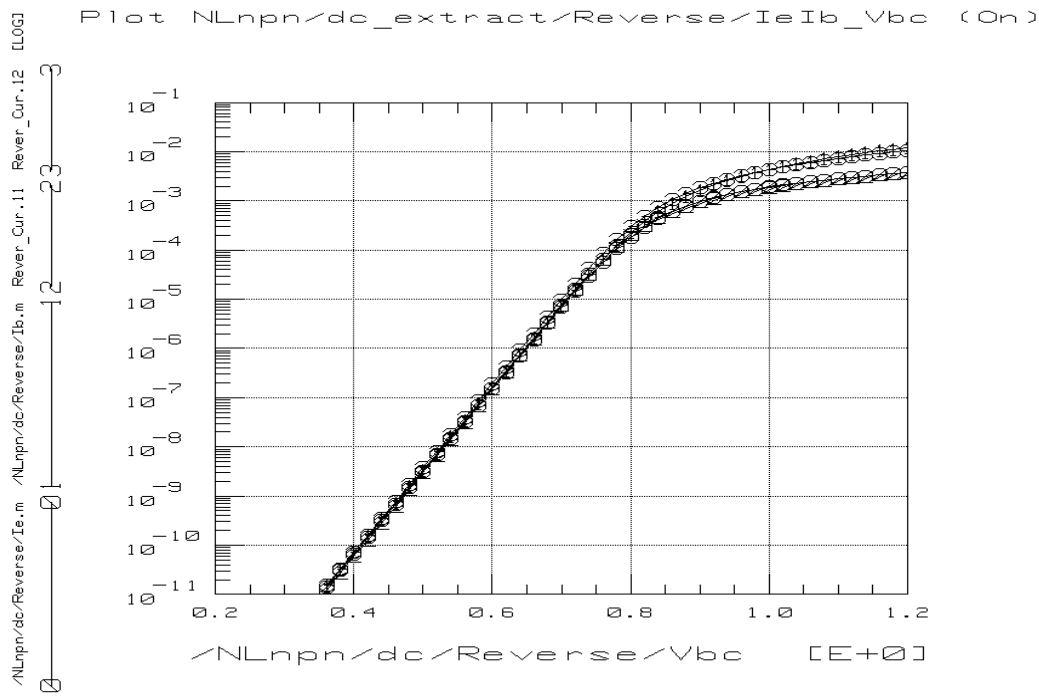


Figure 13: Measured and simulated emitter and base current of the reverse Gummel plot. The value of extracted parameters are:  $RCC = 14.9\Omega$ ,  $XEXT = 0.352$  and  $IKS = 6.64mA$ .

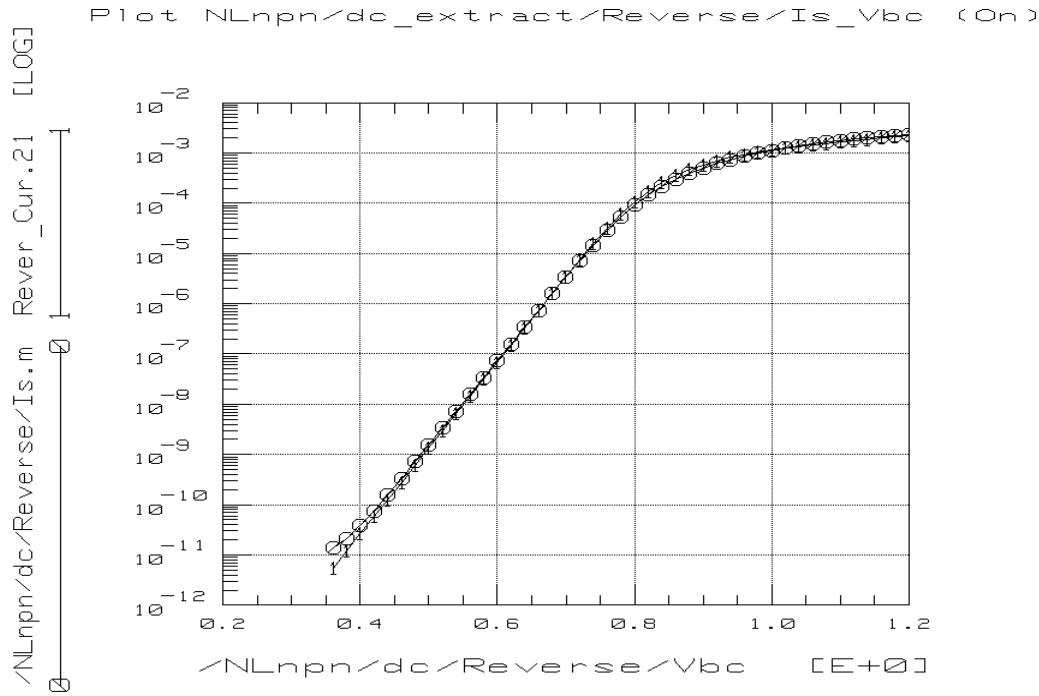


Figure 14: Measured and simulated substrate current of the reverse Gummel plot.

When the emitter resistance  $RE$  and the temperature scaling parameters are known, the increase of the temperature can be obtained from the measured  $V_{be}$  by examining different values for the thermal resistance  $R_{therm}$ ,

$$\Delta T = R_{therm} \cdot I_c \cdot V_{ce}$$

Typical values found for  $R_{therm}$  are between 100 – 400 °C/W.

The epilayer parameters  $RCV$ ,  $SCRCV$ ,  $IHC$ ,  $VDC$  and the knee current  $IK$  may be obtained from the output characteristics. In many cases only  $RCV$ ,  $SCRCV$  and  $IK$  can be extracted in a reliable way. Then the critical current for hot-carriers  $IHC \approx q \cdot N_{epi} \cdot A_{em} \cdot v_{sat}$  and the collector diffusion voltage  $VDC \approx V_t \cdot \ln(N_{epi}/n_i^2)$  are calculated from the epilayer dope and the emitter area. An alternative way is to extract  $RCV$  from the cut-off frequency  $fT$ . At small values of  $V_{cb}$  the collector current where the  $fT$  has its maximum strongly depends on  $RCV$ . The results become even better if we measure  $fT$  versus  $I_c$  with forward biased base-collector junction e.g.  $V_{cb} = -300mV$ . The extracted epilayer resistance will be close to:  $RCV = (V_{dc} + V_{cb})/I_c(fT_{max})$ . Current spreading in the collector epilayer increases  $IHC$  and decreases the ohmic resistance  $RCV$  and the space charge resistance  $SCRCV$ .

The description of the main current  $I_n$  and the epilayer current  $I_{c_1c_2}$  resulting into  $I_c$  are the relevant parts of the MEXTRAM model that describes the quasi-saturation and the forward mode of operation:

$$I_c = \frac{IS_T \cdot \left( \exp\left(\frac{V_{b_2e_1}}{V_T}\right) - \exp\left(\frac{V_{b_2c_2}}{V_T}\right) \right)}{1 + \frac{Q_{te} + Q_{tc} + Q_{be} + Q_{bc}}{QBO_T}} \quad (45)$$

where from [1]  $Q_{te}$ ,  $Q_{tc}$ ,  $Q_{be}$  and  $Q_{bc}$  are given by equations 2.74, 2.80, 2.87 and 2.89 respectively. The elements of equation 45 are a function of the internal junction voltages  $V_{b_2e_1}$ ,  $V_{b_2c_2}$  and  $V_{b_2c_1}$ . The voltage  $V_{b_2e_1}$  can simply be calculated from the applied base current  $I_b$  when we neglect the non-ideal base current, the extrinsic collector junction is reverse biased, and there is no generation of avalanche current,

$$V_{b_2e_1} = V_t \cdot \ln\left(\frac{BF_T \cdot I_b}{IS_T}\right) \quad (46)$$

Normally the non-ideal base current is small at these high currents. It can be included in the calculation of  $V_{b_2e_1}$  and then  $V_{b_2e_1}$  has to be solved in an iterative way. The avalanche current  $I_{avl}$  generated at high collector voltages adds up to the supplied base-emitter current in this measurement setup. To avoid the complex calculation of  $I_{avl}$  we exclude these data points from the parameter extraction.

From the measured value of  $I_c$  and  $I_b$  we can calculate the junction voltage  $V_{b_2c_1}$ ,

$$V_{b_2c_1} = V_{b_2e_1} + I_c \cdot RCC_T + (I_b + I_c) \cdot RE - V_{ce} \quad (47)$$

The junction voltages  $V_{b_2e_1}$  and  $V_{b_2c_1}$  can be calculated in pre-processing. The most internal base-collector junction voltage  $V_{b_2c_2}$  is solved by applying the Kirchoff law

to node  $c_2$  of the equivalent circuit,

$$I_n = I_{c_1 c_2}$$

where  $I_{c_1 c_2}$  is the current through the epilayer and is defined in [1] by eqn. 2.68. Fitting the measured collector current to  $I_n$  the unknown parameters ( $IK$ ,  $RCV$ ,  $SCRCV$ ,  $VDC$  and  $IHC$ ) in the equations of  $I_n$  and  $I_{c_1 c_2}$  can be extracted. We have to be careful about the extracted value of the knee current  $IK$ . In the MEXTRAM model the base transit time  $\tau_b$  is proportional with  $QB0/IK$ . When the extracted  $IK$  is too small, the base transit time becomes too large and may be larger than the total transit time computed from the maximum value of the cut-off frequency. Therefore  $\tau_b < \frac{1}{2 \cdot \pi \cdot fT_{max}}$ . This condition sets a minimum value for  $IK$ ,

$$IK_{min} \approx (10 \dots 20) \cdot fT_{max} \cdot QB0 \quad (48)$$

An example of the output characteristics is shown in figure 15.

Input function	: $V_{ce}$ , $I_c$ and $I_b$
Output function	: $I_c$
Extracted parameters	: $IK$ , $RCV$ , $SCRCV$ ( $VDC$ , $IHC$ )
Approximations	: non-ideal base current neglected ( $I_{b2} \ll I_b$ ) no avalanche ( $I_{avl} \ll I_b$ ) no hard saturation ( $I_{ex}$ and $I_{sub} \ll I_b$ )
Option	: account for self-heating when $R_{therm} > 0$ .

## 18 Cut-off frequency $fT$

In this measurement setup the cut-off frequency  $fT$  is obtained from S-parameter measurements in the common emitter configuration. We measure  $fT$  at 3 constant DC values of  $V_{cb}$  as a function of the base-emitter voltage  $V_{be}$ . For sufficient high frequencies the measured cut-off frequency becomes;

$$fT = freq \cdot \left| \frac{i_c}{i_b} \right| = freq \cdot \left| \frac{Y_{21}}{Y_{11}} \right| \quad (49)$$

An alternative way is to measure the  $fT$  at medium frequencies as follows;

$$fT = \frac{freq}{imag(i_b/i_c)}$$

The difference between both methods is that we extrapolate in the first method at high frequencies in the roll-off region of the AC current gain and in the second method we use the data point at medium frequencies where the AC current gain is constant. The advantage of the second method is that for high frequency transistor the validity range is larger. The frequency should be sufficient high to measure accurately  $imag(i_b/i_c)$ .

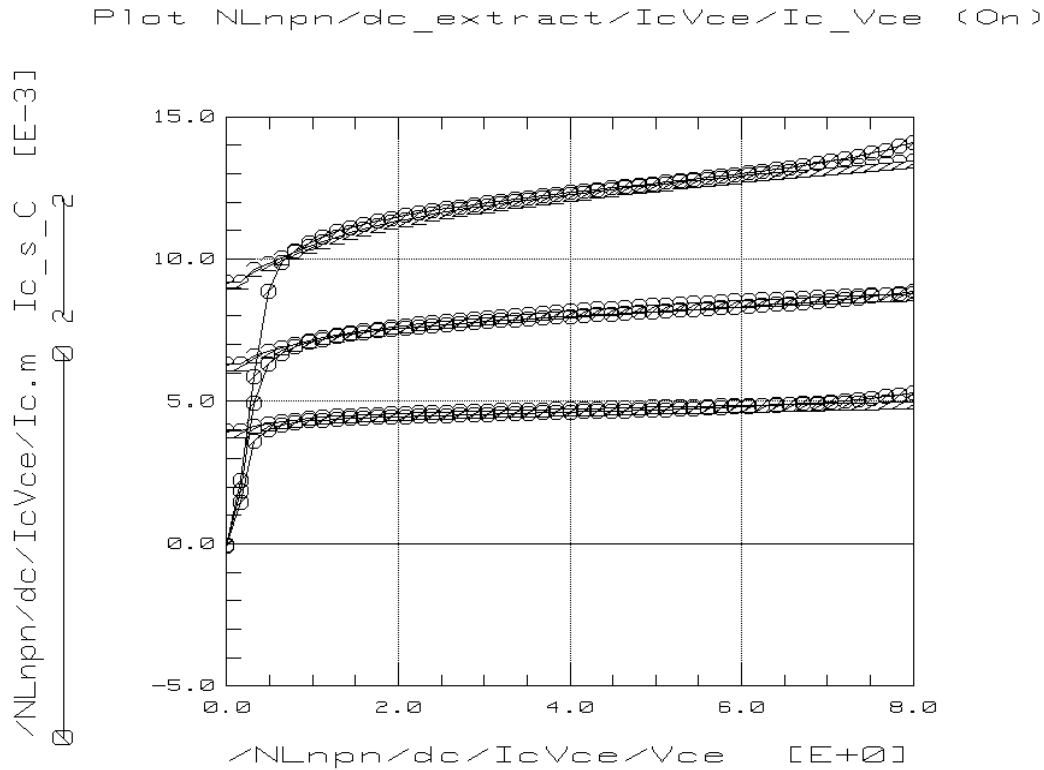


Figure 15: Measured and simulated output characteristics. The hard saturation region  $V_{ce} < 0.5V$  and the region where avalanche multiplication is present  $V_{ce} > 6V$  are excluded from the optimization range. The value of extracted parameter  $SCRCV = 1.64k\Omega$ . For this transistor the knee current  $IK$  is approximately  $50mA$ . Due to this high value it can not be extracted from the output characteristic. The calculated ohmic resistance  $RCV = 120\Omega$  and the diffusion voltage  $V_{dc} = 650mV$ .

The simulated cut-off frequency is calculated in a different way:

$$fT = \frac{1}{2 \cdot \pi \cdot \tau} \quad (50)$$

where  $\tau$  is the total emitter–collector transit time defined as,

$$\tau = \left. \frac{dQ}{dIc} \right|_{dV_{ce}=0} \quad (51)$$

The total differential charge  $dQ$ , the differential current  $dIc$  with shorted collector,  $dV_{ce} = 0$ , are calculated analytically as a function of the two internal junction voltages  $V_{b_2e_1}$  and  $V_{b_2c_2}$  in this way,

$$\begin{aligned} dQ &= \frac{\partial Q}{\partial V_{b_2e_1}} \cdot dV_{b_2e_1} + \frac{\partial Q}{\partial V_{b_2c_2}} \cdot dV_{b_2c_2} \\ dIc &= \frac{\partial Ic}{\partial V_{b_2e_1}} \cdot dV_{b_2e_1} + \frac{\partial Ic}{\partial V_{b_2c_2}} \cdot dV_{b_2c_2} \end{aligned}$$

$$dV_{ce} = \frac{\partial V_{ce}}{\partial V_{b_2e_1}} \cdot dV_{b_2e_1} + \frac{\partial V_{ce}}{\partial V_{b_2c_2}} \cdot dV_{b_2c_2} = 0$$

After substitution of these differential equations in (51) the emitter–collector transit time  $\tau$  becomes,

$$\tau = \frac{\frac{\partial Q}{\partial V_{b_2e_1}} - \frac{\partial Q}{\partial V_{b_2c_2}} \cdot \frac{\frac{\partial V_{ce}}{\partial V_{b_2e_1}}}{\frac{\partial V_{ce}}{\partial V_{b_2c_2}}}}{\frac{\partial I_c}{\partial V_{b_2e_1}} - \frac{\partial I_c}{\partial V_{b_2c_2}} \cdot \frac{\frac{\partial V_{b_2e_1}}{\partial V_{ce}}}{\frac{\partial V_{b_2c_2}}{\partial V_{ce}}}} \quad (52)$$

The complexity of the calculation of the transit time reduces considerable when we exclude the quasi-saturation regime. For the purpose of parameter extraction this is reasonable because the cut-off frequency has already passed its maximum when the transistor comes into quasi-saturation. During parameter extraction only the  $fT$  up to the maximum has to be fitted to obtain the neutral emitter transit time parameters  $TAUNE$  and  $MTAU$ . In many cases we find for the non-ideality factor  $MTAU = 1$ . To calculate the cut-off frequency in the quasi-saturation regime small signal Y parameters has to be simulated with an external linked circuit simulator with the MEXTRAM model implemented. In general for circuit-simulation purposes a good description of the cut-off frequency up to and not so far exceeding its maximum is sufficient. Therefore we try to obtain the epilayer parameters from the output characteristics and extract only the  $TAUNE$  parameter from the measured  $fT$  to fit its maximum. The measured  $fT$  data at the three different  $V_{cb}$  values are also used to check the overall quality of the extracted parameter set ( $V_{cb}$  dependency), because many of the extracted model parameters directly contribute to the total transit time and therefore the cut-off frequency.

In the solution procedure first the bias operating point of the transistor has to be calculated and in the next step all the partial derivatives of the charges, currents and voltages at this operating point. The transistor is biased with the base-emitter voltage and the base-collector voltage. The measured collector current, without quasi-saturation ( $Q_{bc} = 0$ ) is,

$$I_c = \frac{IS_T \cdot \exp\left(\frac{V_{b_2e_1}}{V_T}\right)}{1 + \frac{Q_{te} + Q_{tc} + Q_{be}}{QBO_T}} \quad (53)$$

where from [1]  $Q_{te}$ ,  $Q_{tc}$  and  $Q_{be}$  are given by equations 2.74, 2.80 and 2.87 respectively. The elements of equation 53 are a function of the internal junction voltages  $V_{b_2e_1}$ ,  $V_{b_2c_2}$  and  $V_{b_2c_1}$ . The two internal base-collector voltages can be calculated as follows,

$$V_{b_2c_1} = V_{bc} + I_c \cdot RCC_T - I_b \cdot RBC_T - V_{b_1b_2} \quad (54)$$

$$V_{b_2c_2} = V_{b_2c_1} + V_{c_1c_2} \quad (55)$$

with

$$I_b = \frac{IS_T}{BF_T} \cdot \exp \frac{V_{b_2e_1}}{V_T} \quad (56)$$

$$V_{b_1b_2} = V_T \cdot \ln \left( 1 + \frac{RBV_T \cdot I_c}{BF_T \cdot V_T} \right) \quad (57)$$

$$V_{c_1c_2} = 0.5 \cdot SCRCV \cdot (I_c - IHC) + \sqrt{(0.5 \cdot SCRCV \cdot (I_c - IHC))^2 + SCRCV \cdot IHC \cdot RCV_T \cdot I_c} \quad (58)$$

The non-ideal part of the base current is neglected. The equation of  $V_{b_1b_2}$  is derived in section 13, equation 32. The voltage drop over the epilayer without quasi-saturation ( $EC = 0$ ) is also given in [1] on page 39. The unknown junction voltage  $V_{b_2e_1}$  is solved in an iterative way. When the calculated voltage  $V_{b_2c_2}$  is greater than the diffusion voltage  $VDC_T$  the cut-off frequency is not computed and set to zero (quasi-saturation regime).

In the next step the partial derivatives of all the charge components connected to the base terminal are calculated with the internal junction voltages  $V_{b_2e_1}$  and  $V_{b_2c_2}$  as being independent,

$$\frac{\partial Q}{\partial V_{b_2e_1}} = \frac{\partial Q_{te}}{\partial V_{b_2e_1}} + \frac{\partial Q_{tc}}{\partial V_{b_2e_1}} + \frac{\partial Q_{be}}{\partial V_{b_2e_1}} + \frac{\partial Q_n}{\partial V_{b_2e_1}} + \frac{\partial Q_{tex}}{\partial V_{b_2e_1}} + \frac{\partial XQ_{tex}}{\partial V_{b_2e_1}} + \frac{\partial Q_{cpe}}{\partial V_{b_2e_1}} + \frac{\partial Q_{cpc}}{\partial V_{b_2e_1}}$$

$$\frac{\partial Q}{\partial V_{b_2c_2}} = \frac{\partial Q_{be}}{\partial V_{b_2c_2}} + \frac{\partial Q_{tc}}{\partial V_{b_2c_2}} + \frac{\partial Q_{tex}}{\partial V_{b_2c_2}} + \frac{\partial XQ_{tex}}{\partial V_{b_2c_2}} + \frac{\partial Q_{cpe}}{\partial V_{b_2c_2}} + \frac{\partial Q_{cpc}}{\partial V_{b_2c_2}}$$

The charges  $Q_n$ ,  $Q_{tex}$  and  $XQ_{tex}$  are given in [1] by equations 2.91, 2.82 and 2.83 respectively. The charges  $Q_{cpe}$  and  $Q_{cpc}$  are parasitic constant capacitances between the base-emitter and base-collector terminal. These capacitances are not part of the MEXTRAM model and added to the equivalent circuit to take into account bound pad and/or envelope capacitances when they are not de-embedded in the  $fT$  measurements.

$$Q_{cpc} = CPBC \cdot V_{bc} \quad (59)$$

$$Q_{cpe} = CPBE \cdot V_{be} \quad (60)$$

Note that the substrate-collector charge  $Q_{ts}$  does not contribute to the emitter-collector transit time. The voltages  $V_{be}$ ,  $V_{b_2c_1}$ ,  $V_{b_1c_1}$ ,  $V_{bc_1}$ ,  $V_{bc}$  and  $V_{ce}$  have to be calculated now as a function of the independent voltages  $V_{b_2e_1}$  and  $V_{b_2c_2}$ ,

$$\begin{aligned} V_{be} &= V_{b_2e_1} + (I_c + I_b) \cdot RE + I_b \cdot RBC_T + V_{b_1b_2} \\ V_{b_2c_1} &= V_{b_2c_2} - V_{c_1c_2} \\ V_{b_1c_1} &= V_{b_2c_1} + V_{b_1b_2} \\ V_{bc_1} &= V_{b_1c_1} + I_b \cdot RBC_T \\ V_{bc} &= V_{bc_1} - I_c \cdot RCC_T \\ V_{ce} &= V_{be} - V_{bc} \end{aligned}$$



In above equations also  $I_c$ ,  $I_b$ ,  $V_{b_1b_2}$  and  $V_{c_1c_2}$  defined by equations (53, 56, 57 and 58) respectively are a function of  $V_{b_2e_1}$  and/or  $V_{b_2c_2}$ . After calculating all the partial derivatives the cut-off frequency is calculated according to equation 50.

- Input function :  $I_c$ ,  $V_{be}$  and  $V_{ce}$
- Output function :  $f_T$
- Extracted parameters :  $TAUNE$ , ( $MTAU$ ,  $MC$ ,  $RCV$ )
- Approximations : non-ideal base current neglected ( $I_{b2} \ll I_b$ )  
 no avalanche ( $I_{avl} \ll I_b$ )  
 no hard- and quasi-saturation,  
 ( $I_{ex} = I_{sub} = I_r = 0$ )  
 $Q_{epi} = Q_{bc} = Q_{ex} = XQ_{ex} = Q_{ts} = 0$
- Options: : constant parasitic capacitances added to account for bound pad and/or envelope capacitances.

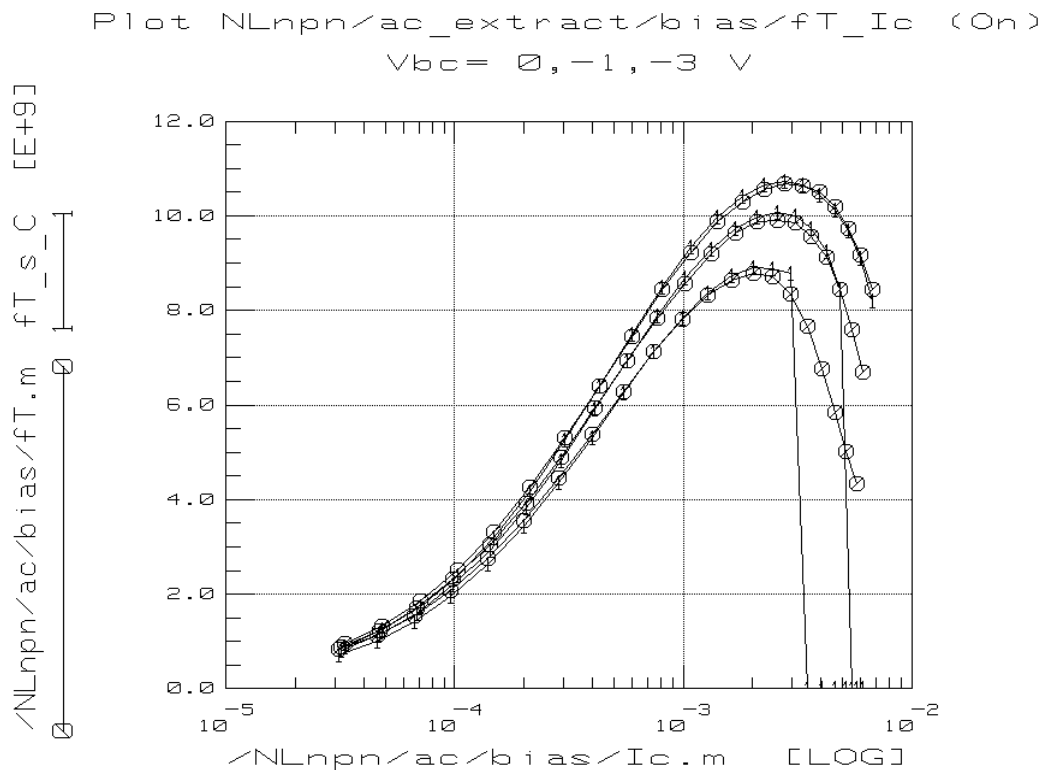


Figure 16: Measured and simulated cut-off frequency  $f_T$ . When the transistor enters quasi-saturation (internal voltage  $V_{b_2c_2} > V_{DC_T}$ ) the simulated  $f_T$  is set to zero. The value of the extracted parameter  $TAUNE = 2.95ps$

## 19 Temperature parameters

In this section the extraction of the parameters in the temperature scaling rules are treated. The MEXTRAM model has 13 parameters dealing with temperature. There are 42 electrical parameters to describe the characteristics at constant temperature of which 20 parameters are temperature independent. Therefore it is not useful to extract all the electrical parameters at different temperatures because also the temperature independent parameters of the individual sets will then varies more or less with temperature. The simplest way to get the parameters of the temperature scaling rules is to repeat only the extraction of the temperature dependent electrical parameters at a higher temperature using the extracted parameter set at the reference temperature as initial set. In this way the temperature independent parameters automatically do not varies with temperature. To verify the scaling rules measurements and simulations may be done at lower and higher temperatures. Because there are more electrical parameters then temperature parameters we have to make choices. The sensitivity of parameters with respect to temperature (large sensitivity gives an easy extraction) and the importance of some characteristics define the choices.

In table 5 a cross reference is given for the temperature parameters and the electrical parameters. In table 6 the cross reference table of the electrical parameters and the temperature parameters is given and finally in table 7 the advised strategy to extract the temperature parameters is given.

1	<i>VGE</i>	<i>BF</i>					
2	<i>VGB</i>	<i>CJE</i>	<i>VDE</i>	<i>IS</i>	<i>BF</i>	<i>QBO</i>	<i>TAUNE</i>
3	<i>VGC</i>	<i>CJC</i>	<i>VDC</i>	<i>XP</i>	<i>IBR</i>	<i>QBO</i>	
4	<i>VGJ</i>	<i>IBF</i>	<i>TAUNE</i>				
5	<i>VI</i>	<i>QBO</i>					
6	<i>NA</i>	<i>QBO</i>					
7	<i>ER</i>	<i>VLf</i>	<i>VLR</i>				
8	<i>AB</i>	<i>IS</i>	<i>IK</i>	<i>BF</i>	<i>RBV</i>	<i>TAUNE</i>	
9	<i>AEPI</i>	<i>RCV</i>					
10	<i>AEX</i>	<i>RBC</i>					
11	<i>AC</i>	<i>RCC</i>					
12	<i>VGS</i>	<i>ISS</i>	<i>CJS</i>	<i>VDS</i>			
13	<i>AS</i>	<i>ISS</i>	<i>IKS</i>				

Table 5: Cross reference table for the temperature and the electrical parameters.

In the first column of table 7 the measurements to be used in the extraction procedure are given. They are named in the same way as in table 4. In table 7 also the related electrical parameters are given who go with the temperature parameters. The extraction sequence is the same as for the electrical parameters except for *QBO*. The reason is that the influence of *QBO* on *IS* is small and therefore *VGB* is hardly effected by the value of *VI* in the temperature scaling rule of *QBO* as contrasted

1	<i>IS</i>	<i>VGB</i>	<i>AB</i>		
2	<i>BF</i>	<i>VGB</i>	<i>AB</i>	<i>VGE</i>	
3	<i>XIBI</i>	–			
4	<i>IBF</i>	<i>VGJ</i>			
5	<i>VLf</i>	<i>ER</i>			
6	<i>IK</i>	<i>AB</i>			
7	<i>BRI</i>	–			
8	<i>IBR</i>	<i>VGC</i>			
9	<i>VLR</i>	<i>ER</i>			
10	<i>XEXT</i>	–			
11	<i>QBO</i>	<i>VGB</i>	<i>VGC</i>	<i>NA</i>	<i>VI</i>
12	<i>ETA</i>	–			
13	<i>AVL</i>	–			
14	<i>EFI</i>	–			
15	<i>IHC</i>	–			
16	<i>RCC</i>	<i>AC</i>			
17	<i>RCV</i>	<i>AEPI</i>			
18	<i>SCRCV</i>	–			
19	<i>SFH</i>	–			
20	<i>RBC</i>	<i>AEX</i>			
21	<i>RBV</i>	<i>AB</i>			
22	<i>RE</i>	–			
23	<i>TAUNE</i>	<i>VGB</i>	<i>VGJ</i>	<i>AB</i>	
24	<i>MTAU</i>	–			
25	<i>CJE</i>	<i>VGB</i>			
26	<i>VDE</i>	<i>VGB</i>			
27	<i>PE</i>	–			
28	<i>XCJE</i>	–			
29	<i>CJC</i>	<i>VGC</i>			
30	<i>VDC</i>	<i>VGC</i>			
31	<i>PC</i>	–			
32	<i>XP</i>	<i>VGC</i>			
33	<i>MC</i>	–			
34	<i>XCJC</i>	–			
35	<i>ISS</i>	<i>VGS</i>	<i>AS</i>		
36	<i>IKS</i>	<i>AS</i>			
37	<i>CJS</i>	<i>VGS</i>			
38	<i>VDS</i>	<i>VGS</i>			
39	<i>PS</i>	–			
40	<i>KF</i>	–			
41	<i>KFN</i>	–			
42	<i>AF</i>	–			

Table 6: Cross reference table for the electrical and the temperature parameters.

Mc	temperature parameter(s)	electrical parameter(s)
	<i>NA</i>	
Cbc	<i>VGC</i>	<i>CJC</i>
Forward	<i>VGB</i>	<i>IS</i>
Vear	<i>VI</i>	<i>QBO</i>
Forward	<i>VGE, ER</i>	<i>BF, VLF</i>
Forward	<i>AEX</i>	<i>RBC</i>
Reverse	<i>VGS</i>	<i>ISS</i>
Reverse	<i>AC, AS</i>	<i>RCC, IKS</i>
IcVce	<i>AEPI, AB</i>	<i>RCV, IK</i>
fT	<i>VGJ</i>	<i>TAUNE</i>

Table 7: Extraction strategy for the temperature parameters.

with the influence of *VGB* on *QBO*. The maximum base dope concentration *NA* and the ionization voltage *VI* determines the temperature dependence of *QBO*. The correlation between *NA* and *VI* is too large to obtain reliable values and therefore in most cases *NA* is set to an appropriate value. Note that the bandgap voltage *VGJ* has to be extracted from the cut off frequency *fT* instead of the non ideal forward base current. Otherwise it can happen that the temperature dependence of *fT* becomes wrong when the origin of the non ideal base current is not due to recombination in the base-emitter depletion region.

Of course other measurements may be used to obtain the temperature parameters depending on transistor type (see table 5). In figure 17 the measured and simulated collector current of the Gummel plot at several temperatures are plotted. In figure 18 the measured and simulated forward current gain are plotted at different temperatures. In both plots only the measurements at the reference (22 degrees celsius) temperature and at 80 degrees are used in the extraction. The curves at 5 and 50 degrees are predicted and compare fairly good with the measurements. This clearly illustrates the physical background of the MEXTRAM temperature scaling rules.

## 20 Summary

The Philips state of the art MEXTRAM bipolar transistor model has been put in the public domain in january 1994. Most of the MEXTRAM transistor parameters can be extracted directly from measured data. We need depletion capacitance (*CV*), Gummel plots, output characteristics, forward and reverse Early and cut-off frequency (*fT*) measurements. To extract parameters of the temperature scaling rules part of the measurements have to be repeated at an other temperature. To determine MEXTRAM transistor parameters the extraction method is implemented in the IC-CAP program of Hewlett Packard. The complete MEXTRAM transistor model is built into the MNS circuit simulator of HP and this simulator can be interfaced with IC-CAP to perform other transistor simulations like DC Gummel plots, output

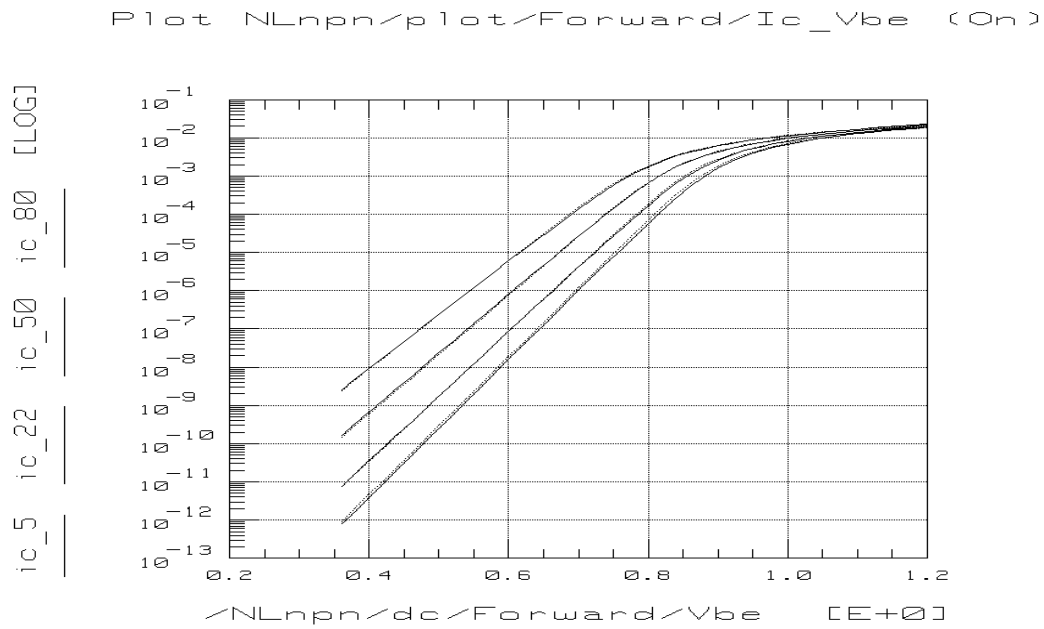


Figure 17: Measured and simulated collector current at 5, 22, 50 and 80 degrees Celsius. The measurements at 22 and 80 degrees are used in the parameter extraction.

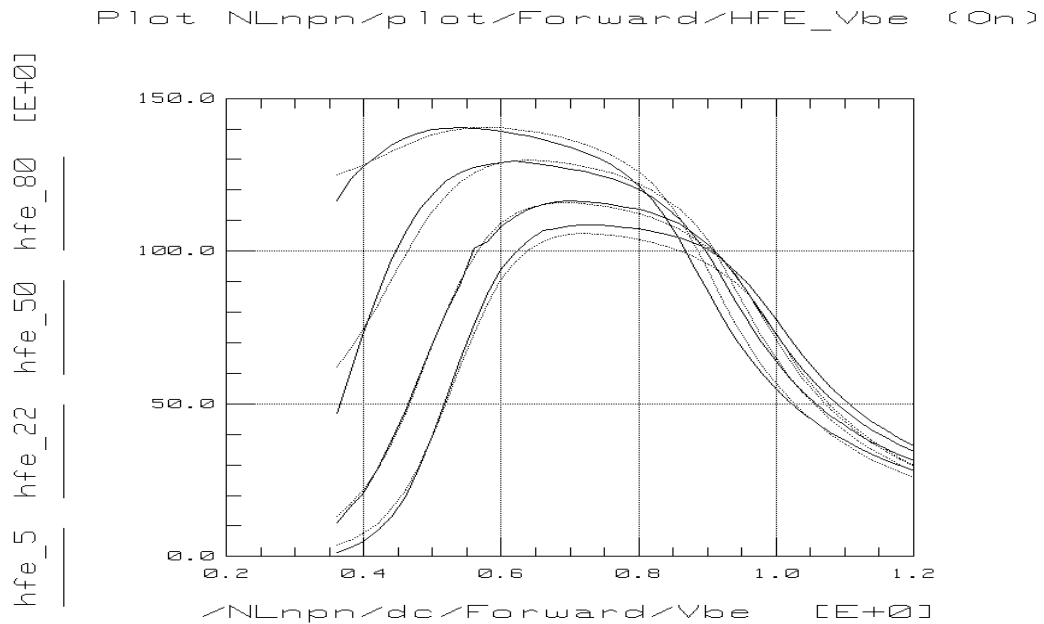


Figure 18: Measured and simulated current gain at 5, 22, 50 and 80 degrees Celsius. The measurements at 22 and 80 degrees are used in the parameter extraction.

characteristics and Y parameters.

To extract reliable transistor parameters it is important that the measurements are done over a large range of collector, base and emitter biasing conditions. The number of data points in an interval is of minor importance. The maximum collector voltage is obtained from the Early forward measurement where the base current becomes negative. Also the collector-base depletion capacitance measurement have to be performed up to this collector voltage. The preferred reverse voltage of the DC Gummel plots is zero volt to avoid avalanche/tunneling currents and self-heating. The output characteristics have to be measured at constant base currents instead of constant base voltage to be less sensitive for self-heating. The collector current has to be sufficient high to exhibit quasi-saturation and/or high injection effects in the output characteristics. The emitter resistance is obtained from the open collector method. In this method the emitter current (and not the base current) is plotted versus the collector voltage. The slope at high emitter current ( $\approx 2mA/\mu m^2$  emitter area) should be more or less constant and be the emitter resistance. The cut-off frequency  $fT$  has to be measured versus collector current at constant values of  $V_{bc}$ . Then base, emitter resistances and self heating has minor influences on the measured characteristics. The preferred  $V_{bc}$  of the first curve is 300 mV to extract accurately the ohmic resistance of the collector epilayer.

The first step in the extraction of model parameters is to generate an initial parameter set. An accurate calculation of the epilayer parameters prevents a lot of troubles and improves the convergency. The general extraction strategy is to put parameters in small groups (typical 1-3) and extract these parameters simultaneously out of measured data sensitive to these parameters (see table 4). In general the optimization of the depletion capacitances (CV), the Early measurements and the forward and reverse gain up to medium current levels will be straight forward. The high current related parameters are extracted from the output characteristics and the cut-off frequency. Here the extraction strategy depend partly on the transistor technology. Transistor having high resistive epilayers (low doped and thick) the high injection knee current of the base is difficult to determine because transistor performance degradation is mainly due to base-push out and the knee current has to be estimated. For very high frequency transistor the epilayer is thin and relative highly doped and now the epilayer resistance is small and difficult to extract. Then in most cases the initially calculated parameters are sufficient accurate.

The determination of the base resistance is derived from the Ning-Tang method. The method fails if the emitter resistance is not sufficient constant (poly-emitter devices with high emitter resistance). The variable part of the base resistance can be fairly calculated when the sheet resistance of the pinched base, the number of base contacts and the emitter dimensions are known.

The MEXTRAM model has 13 parameters dealing with temperature. The simplest way to get the parameters of the temperature scaling rules is to repeat only the extraction of the temperature dependent electrical parameter at a higher temperature using the extracted parameter set at the reference temperature as initial set. To

verify the scaling rules measurements and simulations may be done at lower and higher temperatures.

To conclude a very fast and accurate parameter extraction method for the bipolar transistor model MEXTRAM has been developed. Using a combination of simplified expressions and selected measurements the the iterative solution of the full model is avoided. This new method greatly enhances the efficiency and user-friendliness of the MEXTRAM parameter extraction.

## References

- [1] H.C. de Graaff and W.J. Kloosterman, Philips Nat. Lab. Unclassified Report Nr. 006/94, "The Mextram Bipolar Transistor Model" level 503.2, June 1995. Request for copies to email address: mm9\_mxt@natlab.research.philips.com
- [2] W.J. Kloosterman, J.A.M. Geelen and D.B.M. Klaassen, "Efficient Parameter Extraction for the Mextram Model". Proceedings of the 1995 Bipolar Circuits and Technology Meeting.



**Author** W.J. Kloosterman and J.A.M. Geelen

**Title** Parameter extraction methodology for the MEXTRAM  
bipolar transistor model

**Distribution**

Nat.Lab./PI

PRL

PL-NAP

LEP

PFL

CP&T

WB-5

Redhill, UK

Briarcliff Manor, USA

Limeil-Brévannes, France

Aachen, BRD

WAH